MATERIALS FOR PHASE HOLOGRAPHIC STORAGE

W. J. Burke, et al

RCA Laboratories

Prepared for:

Office of Naval Research

April 1975

UNCLASSIFIED

SECURITY CLASSIFICATION OF THIS PAGE (When Data Entered)

REPORT DOCUMENTATION PAGE

READ INSTRUCTIONS BEFORE COMPLETING FORM

1. REPORT NUMBER	2. GOVT ACCESSION NO. / 3. RECIPIENT'S CATALOG NUMBER
4. TITLE (and Subtitle): MATERIAL FOR PHASE HOLOGRAPHIC STORAGE	5. TYPE OF REPORT & PERIOD COVERED: Final Report (1-1-74 to 12-31-74)
	6. PERFORMING ORG. REPORT NUMBER: PRRL-75-CR-21
7. AUTHOR(s): William Burke, William Phillips, David L. Staebler, and Brown F. Williams	8. CONTRACT OR GRANT NUMBER(s): N00019-74-C-0312
9. PERFORMING ORGANIZATION NAME AND ADDRESS: RCA Laboratories, Princeton, New Jersey 08540	10. PROGRAM ELEMENT, PROJECT, TASK AREA & WORK UNIT NUMBERS
11. CONTROLLING OFFICE NAME AND ADDRESS: Naval Air Systems Command, Department of the Navy, Washington, D.C. 20361	12. REPORT DATE: April 1975 / 13. NUMBER OF PAGES: 72
14. MONITORING AGENCY NAME & ADDRESS (if different from Controlling Office)	15. SECURITY CLASS. (of this report): Unclassified / 15a. DECLASSIFICATION/DOWNGRADING SCHEDULE: N/A

16. DISTRIBUTION STATEMENT (of this Report)

17. DISTRIBUTION STATEMENT (of the abstract entered in Block 20, if different from Report)

APPROVED FOR PUBLIC RELEASE; DISTRIBUTION UNLIMITED

18. SUPPLEMENTARY NOTES

19. KEY WORDS (Continue on reverse side if necessary and identify by block number)

Phase holographic storage
Fe-doped $LiNbO_3$

20. ABSTRACT (Continue on reverse side if necessary and identify by block number)

This report describes the results of our effort to develop a better understanding of the recording, erasure, and fixing behavior of Fe-doped $LiNbO_3$ at elevated temperatures and development of methods to improve the material performance. The major results of this study were:

(a) The drift-like nature of the recording process at elevated temperatures was confirmed and a model to explain this effect was developed from studies of the bulk photovoltaic effect.

DD FORM 1 JAN 73 1473 EDITION OF 1 NOV 65 IS OBSOLETE

UNCLASSIFIED

SECURITY CLASSIFICATION OF THIS PAGE (When Data Entered)

20.

(b) A model for the hologram erasure process at elevated temperatures was developed and tested.

(c) The identification of Si as a mobile ionic species which may contribute to the fixing of holograms in Fe-doped $LiNbO_3$.

(d) The discovery that in Mn-doped $LiNbO_3$ the recording sensitivity increases by a factor of fifty at 120°C as compared with that at room temperature.

These results have led to an understanding in detail of the mechanisms of hologram storage in $LiNbO_3$. This understanding has led to the development of techniques for the permanent storage of 500 holograms with ~5% efficiency in Fe-doped $LiNbO_3$ and point the way to increases in capacity which make the Fe-$LiNbO_3$ recording system limited only by fundamental optical principles, not material parameters.

PREFACE

This report describes work performed during the period January 1, 1974 to December 31, 1974 in the Physical Electronics Research Laboratory of RCA Laboratories under Contract No. N00019-74-C-0312. G. Cody is the Laboratory Director, and B. F. Williams is the Group Head. The Project Scientist is B. F. Williams. W. Burke, W. Phillips, and D. L. Stabler participated in the research.

The Government Project Monitor is James Willis.

TABLE OF CONTENTS

LIST OF ILLUSTRATIONS

LIST OF ILLUSTRATIONS (Continued)

SECTION I

INTRODUCTION

Holographic techniques and materials for the storage of information have been extensively developed during the past decade. This effort has been primarily on thin storage media such as photoresists and other materials which can exhibit surface relief or on photographic film which is typically several times thicker than a wavelength of light. In a number of applications thick storage media are preferable because of their capacity for high-density storage of information. (The thickness is on the order of millimeters as opposed to ∿10 μm for photographic film). In this case holograms are stored throughout the bulk of the medium and a given hologram is read out only when Bragg condition for constructive interference is satisfied. Using this angular selectivity, the theoretical limit for bulk optical storage, bit volumes on the order of λ^3, can be approached. The work on thick-phase holography has not been as extensive until now since materials with the requisite high sensitivity and diffraction efficiency have not been available.

In past programs at RCA Laboratories with the support of the Navy a volume phase holographic storage medium based upon Fe-doped $LiNbO_3$ has been developed. Fe-doped $LiNbO_3$ possesses all the requirements for such a storage medium, i.e., high recording sensitivity, high diffraction efficiency, and erasure resistance. The current capabilities of Fe-doped $LiNbO_3$ are:

(a) Availability of crystals with excellent optical quality,
(b) Capability for hologram fixing with a simple heat treatment,
(c) Good sensitivity (∿10 J/cm^2 of 4880 Å light for a fixed hologram of ∿40% diffraction efficiency), and
(d) Good storage capacity (over 500 completely fixed holograms have already been recorded in one cyrstal).

Holograms in Fe-doped $LiNbO_3$ arise from optical excitation and subsequent redistribution of electrons trapped at Fe impurity sites [1]. This sets up a space-charge field that modulates the refractive index via the electro-optic

1. D. L. Staebler, W. Phillips, and B. W. Faughnan, *Materials for Phase Holographic Storage (U)*, Final Report, Contract N00019-72-C-0147, prepared for Naval Air Systems Command, March 1973.

effect. Fixing of the recorded holograms is accomplished by thermally activated ionic motion. When a crystal is heated, increased ionic conductivity tends to neutralize the electronic space-charge patterns and ionic charge-patterns are formed which are replicas of the original holograms. Upon cooling to room temperature, the ionic patterns are stabilized. When the electrons are partially redistributed by light, a net space-charge pattern appears, and the fixed hologram can be read out. This model was first developed to describe fixing in undoped $LiNbO_3$ but is also applicable to Fe-doped crystals.

In an earlier device research program it was discovered that recording and fixing could be accomplished at the same time if the holograms were recorded at elevated temperatures. It was found that for Fe-doped $LiNbO_3$ the optimum recording temperature was 160°C. The purpose of the present program was to develop a more complete understanding of the recording, erasing, and fixing behavior of Fe-doped $LiNbO_3$ at the elevated recording temperature.

This report is organized into seven sections. Section II describes measurements on the storage, erasure, and fixing behavior of Fe-doped $LiNbO_3$ at elevated temperatures. Section III describes our measurements of the bulk photovoltaic effect in this medium and a model for this effect. This model accounts for the apparent internal field observed in Fe-doped crystals during recording. Section IV describes both the experiments by which Si was identified as the mobile ionic species and the implications of this discovery. Section V contains experimental results on increased multiple storage capacity with increasing Fe concentration and a model for this increase based upon the photovoltaic studies. In Section VI we discuss our results for other dopants and in particular for Mn where thermally activated recording sensitivity is observed. Section VII contains the summary and conclusions of this report.

SECTION II

HIGH TEMPERATURE STUDIES

Previous studies under our materials research program have led to the development of Fe-doped $LiNbO_3$ for holographic storage of images and to an understanding of the properties of this material at room temperature [1,2]. These studies have also shown that optimum performance for multiple storage applications is obtained when the holograms are recorded at high temperatures (T ~160°C) [3]. During the current contract period we have studied the behavior of crystals of Fe-doped $LiNbO_3$ at high temperatures for two reasons:

(1) To determine the best operating conditions for storage and erasure of fixed holograms and

(2) To develop a more complete model for the processes involved.

In this section of the report the effect of high-temperature recording on the writing, fixing, and erasure behavior will be discussed.

A. STORAGE

The model developed at RCA Laboratories to describe the recording process in Fe-doped $LiNbO_3$ at room temperature showed that an internal electric field or another mechanism whose effect was identical to that of an internal field was present in the crystal. The effect of such a field is to increase the recording sensitivity. The presence of this internal field was clearly shown by recording characteristics which could only be explained by electron drift and by the observation that an external field applied in the -c direction caused the recording sensitivity to decrease [2]. Correspondingly a field applied in the +c direction produced an increase in the recording sensitivity.

---

2. D. L. Staebler, W. Phillips, W. Burke, and B. W. Faughnan, *Materials for Phase Holographic Storage (U)*, Final Report, Contract N00019-73-C-0273, prepared for Naval Air Systems Command, February 1974.
3. W. Burke and D. L. Staebler, *Volume Holographic Material Device Feasibility for Map Display Applications*, Final Report, Contract N62269-72-C-0793, prepared for Naval Air Development Center, June 1973.

At high temperatures ionic motion will relax the long-range internal field in the same manner as it relaxes the short range fields associated with the holographic grating. In this case the recording sensitivity should decrease. Instead it increased by a factor of two [2].

In order to better understand the recording process, the electro-optic effect and the recording sensitivity in the presence of an applied field at high temperatures were studied. A sample of Fe-doped $LiNbO_3$ was mounted on a resistive heater consisting of a thin slab of insulating alumina with a deposited molybdenum heater on the side opposite the sample. A hole drilled in the center of the heater provided access for hologram readout. Collodial graphite contacts on the + and - c sides of the sample were used to apply the electric field. The presence of the field was verified by watching its effect on the sample's birefringence. This was done by setting up the system between two crossed polarizers and monitoring the amount of transmitted laser light. The strength of the applied field (for a given voltage) was found by this technique to be independent of its polarity. The same was true for the measured current (see Section III).

The storage sensitivity was measured by recording a hologram using a HeNe laser and reading it out with one of the recording beams. Care was taken to keep the storage time shorter than the ionic relaxation time (see subsection B below) to ensure that the entire hologram could be observed upon readout. The results are shown in Fig. 1. The same kind of asymmetric behavior that occurs at room temperature is seen: decrease of sensitivity for one polarity, increase for the other. Clearly, the driving force contributing to the drift-like effect in our crystals is still present at the elevated temperature and is not relaxed via ionic motion. In Section III the origin of this drift-like effect will be discussed in terms of the results of photocurrent experiments and a model for this effect suggested.

B. HOLOGRAM FIXING

Hologram fixing in $LiNbO_3$ occurs via drift of mobile ions in the electronic space-charge field of the original holographic grating [4]. The drift of these

4. D. L. Staebler and J. J. Amodei, Ferroelectrics 3, 107 (1972).

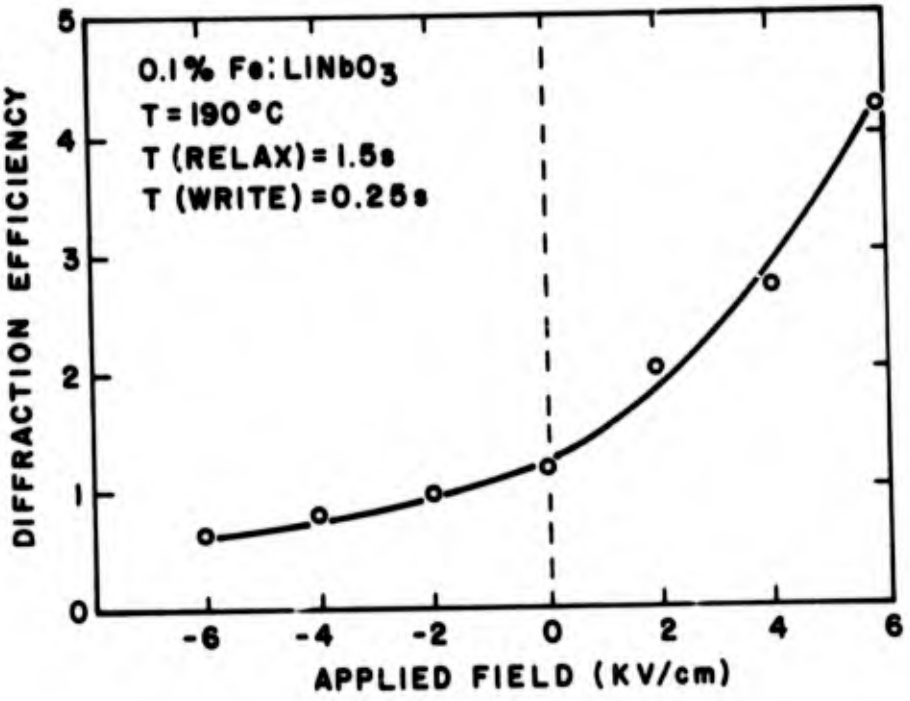

Figure 1. Relative storage sensitivity as a function of applied field. [Each point is the diffraction efficiency produced by the same storage pulse. The relatively fast ionic relaxation time (~1.5 s) is expected to erase any internally generated electric fields.]

ions produces an ionic space-charge pattern which is a replica of the electronic charge pattern. Subsequent uniform redistribution of the trapped electrons leaves only the ionic charge pattern which modulates the index of refraction through the electro-optic effect thus producing a light-insensitive phase grating. Silicon ions have been identified as the mobile ions by means of photocoloration experiments which are discussed in detail in Section V of this report.

To confirm that the same relaxation process occurs in Fe-doped and undoped crystals, the ionic conductivity as measured directly was compared with that from holographic compensation by space-charge relaxation.

The ionic conductivity was measured using the apparatus described in subsection A above for a 0.1% Fe-doped $LiNbO_3$ crystal. The conductivity was measured directly using an applied external field. The results are shown in Fig. 2.

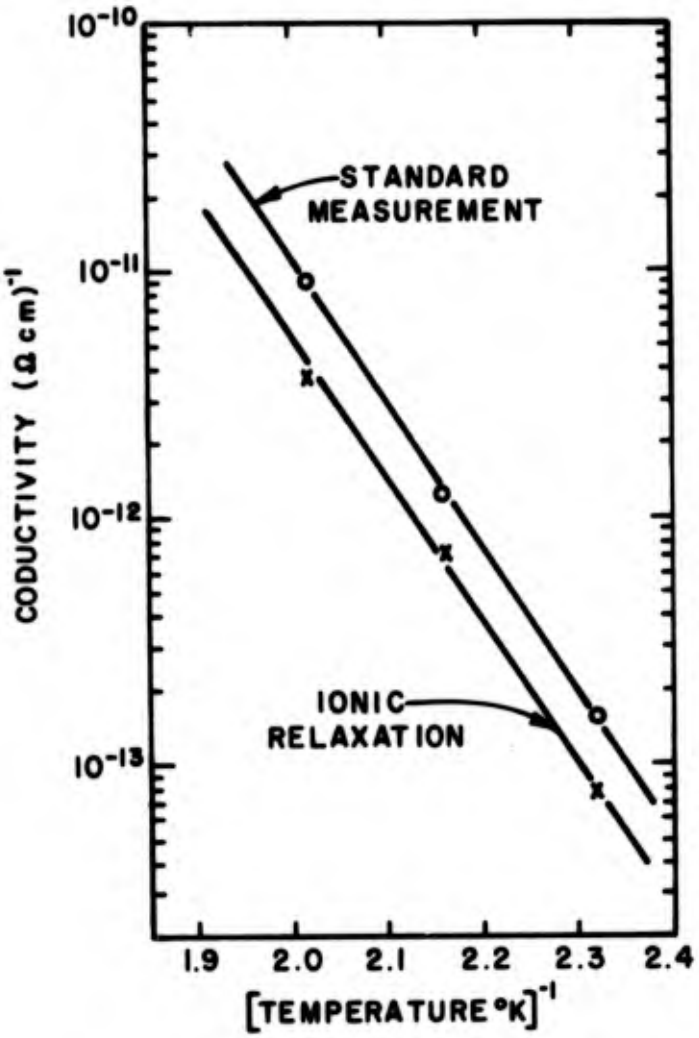

Figure 2. Conductivity as a function of temperature for a 0.1% Fe-doped crystal measured by two different techniques.

Space-charge relaxation is an exponential process with a characteristic time constant τ [5]:

$$\tau = \varepsilon/\sigma \tag{1}$$

where ε is the static dielectric constant and σ is the ionic conductivity. A measurement of the dielectric relaxation via ionic compensation of a hologram will give a value for the ionic conductivity which can be compared with the direct measurement. The efficiency η of a hologram is

5. For example, Shyh Wang, *Solid State Electronics* (McGraw-Hill, New York, 1966), p. 274.

$$\eta \propto E^2 = E_o^2 \, e^{-2t/\tau} \qquad (2)$$

where E is the electronic space-charge field and E_o is its initial value. Therefore, the measured time constant is equal to one-half of the dielectric relaxation time. The results of this measurement are also shown in Fig. 2.

From Fig. 2 we see that the two measurements agree within a factor of two, and since the two lines are parallel, they possess the same activation energy. From the slopes of these lines, an activation energy of 1.18 eV is obtained which is identical with the results for undoped crystals [4]. These results indicate that the fixing mechanism is the same in both cases and that, from the well-defined activation energies, the ionic species is also the same in both cases.

C. THERMAL ERASURE

In an earlier device program, thermal erasure was observed to be a serious problem in the storage of large numbers of holograms [3]. This effect served to limit the number of holograms with useable diffraction efficiency which could be stored in a crystal. We have obtained significantly improved results which will be discussed in Section III of this report. Here we present the results of a detailed study of thermal erasure. A model for the erasure process and the conditions for optimal performance (Fe concentration, grating spacing, and temperature) are discussed.

The erasure studies were made by recording a hologram at an elevated temperature, letting it quickly relax by the ionic process described above and then monitoring the extremely weak readout ($\sim$0.1% diffraction efficiency) that remains. This is probably an absorption hologram associated with the redistribution of the trapped (and absorbing) electrons. We confirmed that the decay of the diffraction efficiency at elevated temperature led to a proportional reduction in the efficiency that could be obtained upon readout of the fixed hologram at room temperature. This experiment was performed at various temperatures using different recording angles (i.e., different grating spacings) and different samples. All samples were prepared by the oxidation/reduction technique described previously [2,6] so that they would have similar absorption properties.

6. W. Phillips and D. L. Staebler, J. Elect. Materials 3, 601 (1974).

Figure 3 shows the results for two different crystals with the indicated nominal dopings. The erasure depends strongly on concentration and grating spacings. For comparison, the ionic relaxation times discussed in subsection B above are also shown in Fig. 3. These are not affected by grating spacings, as is expected for a relaxation process, and show no consistent dependence on doping. The only difference in the fixing rate from crystal to crystal is that due to slight variations in the ionic conductivity [4].

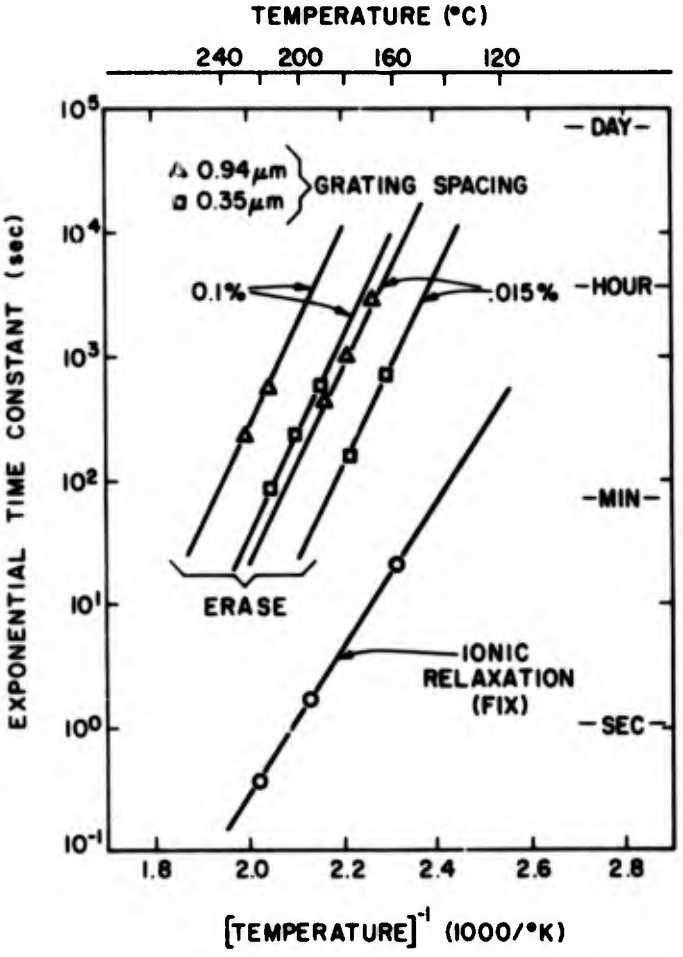

Figure 3. Thermal time constants for erasure of fixed holograms. The grating spacing depends on the wavelength and the angle between the beams. [This was done at 4880 Å with beam angles of 30° (0.94 μm) and 90° (0.35 μm). Also shown are the fixing times.]

The region of interest in Fig. 3 is between the fix and erase lines. Only here can one record a fixed hologram. (In principle, one can record a hologram in a time shorter than the fixing time and then let it slowly fix as another is being recorded. However, this approach will probably produce optical erasure and optical damage problems [7]. The preferred situation is to record the holograms at the lowest possible temperature and to use heavily doped crystals and long grating spacings to obtain a long erasure time. Our experiments have generally involved recording holograms at ∿160°C, the temperature at which the fixing time is roughly equal to the storage time. Here, our results (see top line in Fig. 3) show that one can obtain an erasure time of more than a day. This time is more than adequate to record 500 to 1000 holograms, the number required for a practical storage system. Note that although longer grating spacings should give longer decay times, this should also decrease the angular selectivity of the holograms. The result would be a smaller storage capacity for a given thickness [3]. The ∿0.94-μm value used here (for storage beams separated by 30°) seems to be a good compromise.

These results strongly confirm the thermal erasure model previously suggested by preliminary work carried out under this program [2]. Erasure is due to diffusion, and subsequent redistribution, of electrons thermally activated from Fe traps.* A solution to the diffusion equation in Appendix A gives the time constant for the decay of the trapped space charge

$$T = \frac{1}{DK^2 g\tau} \tag{3}$$

where D is the diffusion constant for electrons, K is the grating constant, g is the generation rate of free electrons per filled trap and has both thermal and optical components, and τ is the lifetime of an electron in the $LiNbO_3$ conduction band.

The agreement between this expanded theory and experiment is excellent. First, the measured variation of erasure time with grating spacing closely follows the quadratic dependence predicted by Eq. (3), e.g., a 0.94-μm grating

7. W. Phillips, J. J. Amodei, and D. L. Staebler, RCA Review 33, 94 (1972).

*The apparent internal field does not affect the erasing rate but shifts the pattern in space inside the crystal as the pattern is erasing by diffusion.

decays ∿7 times slower than a 0.35-μm grating. Second, the temperature and concentrations variations of the decay time are explained entirely by variations of g and τ in Eq. (3), respectively. The temperature variation of the decay time can be used to measure the activation energy for the generation of trapped electrons [see Eq. (2)]. From the slope of the erasure lines in Fig. 3 we find an activation energy of ∿1.48 eV, quite similar to that measured for thermal ionization of Fe^{2+} ions in photochromic $LiNbO_3$.

The effect of the Fe concentration is associated with τ, the lifetime. The lifetime depends, in part, on the concentration of empty traps. Increasing this concentration by putting more Fe into the crystal will decrease the lifetime. This will then lead to longer erase times, as we observe in Fig. 3. This model predicts that the increase in erase time will be proportional to the increase in the Fe-doping level. EPR measurements on the samples used for Fig. 3 show a factor of ten difference in Fe^{3+} concentration, in fair agreement with our results.

To check this, we also measured the room temperature optical erasure of unfixed holograms in these crystals. The results are shown in Fig. 4. The heavily doped crystals have an erasure sensitivity ∿10 times lower than the other one, consistent with the lifetime model discussed above. Here at the lower temperature, however, the erasure is due to dielectric relaxation, and the lifetime affects the erasure through its effect on the photoconductivity [8].

D. CONCLUSIONS

From the results presented above it is clear that the recording properties of Fe-doped $LiNbO_3$ at high temperatures are essentially the same as at room temperature with the addition of a thermal erasure component to the optical erasure present at room temperature. Thermal erasure occurs via thermal ionization and diffusion of trapped electrons. The predictions of this model were found to agree quite well with experiment. Fixing of a hologram via thermally activated ionic motion was found to occur in an identical manner in Fe-doped and "pure" $LiNbO_3$.

---

8. D. L. Staebler and W. Phillips, Appl. Opt. 13, 788 (1974).

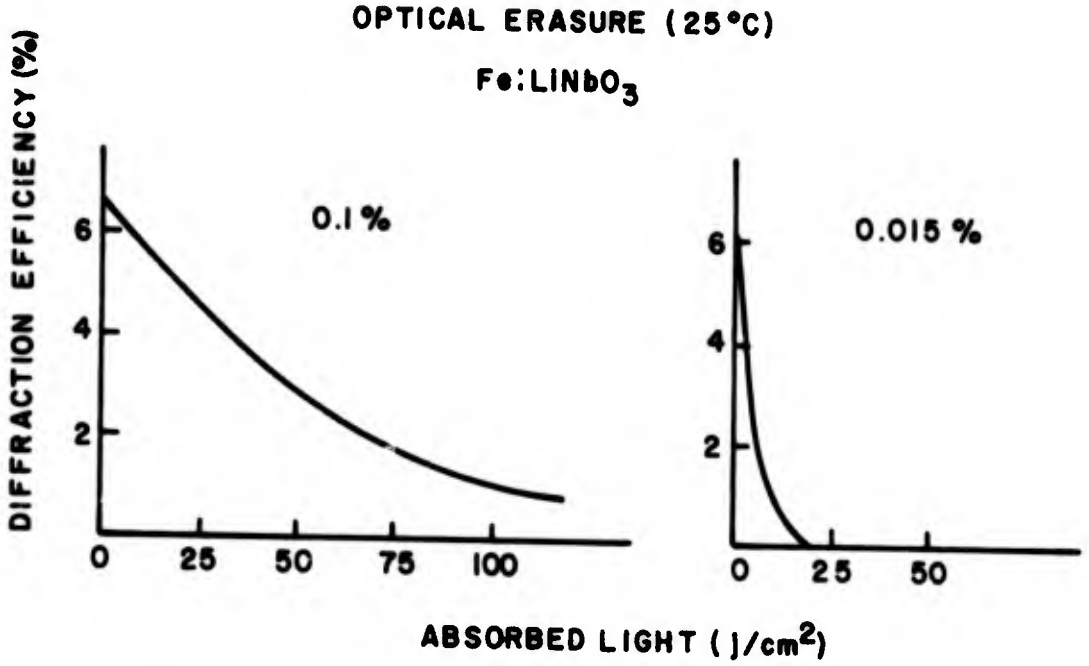

Figure 4. Optical erasure of the two crystals used for the data of Fig. 3. The results corroborate the model that the fast thermal erasure of the low-doped crystal is due to longer free carrier lifetimes.

It is also clear that at the recording temperature an effect exists in the crystal which can be treated formally as an internal electric field. A true electric field cannot exist since it would be relaxed by ionic motion. A model to explain this effect will be presented in Section III in the context of the discussion of our experiments of photocoloration and photocurrents.

SECTION III

HOLOGRAM STORAGE MODEL

As originally developed under this program, the model for the greatly improved storage sensitivity in Fe-doped crystals (as compared with undoped crystals) had two distinct aspects. First, the Fe impurities provide electron traps suitable for a storage process. The filled traps (Fe^{2+} ions) absorb the incident light and thereby generate free electrons. The electrons move and are retrapped at empty traps (Fe^{3+} ions), thereby creating a space-charge pattern. Secondly, the presence of the Fe impurities is thought to produce a strong ($\sim 10^4$ V/cm) internal field that moves the free carriers via drift. The role of the Fe as electron traps in thermal and optical erasure was discussed in Section II. On the other hand, the role of the traps in the generation of an internal field has never been explained. The only piece of evidence has been that a drift mechanism for storage is observed only for crystals that contain more than 10^{18} cm^{-3} empty traps (i.e., heavily doped crystals). For crystals with fewer Fe^{3+} ions, diffusion is the predominant mechanism for storage. These mechanisms were established by coupled wave measurements, studies of the effect of applied fields on the storage sensitivity, and comparison of the storage sensitivity with the erase sensitivity.

The problem with this model was that the same behavior is observed at elevated temperatures where ionic transport should relax any internal field. In this section we present some new results on the storage process and discuss a model which explains the drift-like behavior observed at both room and elevated temperatures.

A. PHOTOINDUCED CURRENTS

Chen [9] found in early studies of $LiNbO_3$ that a photocurrent could be produced without an applied voltage; he related this current to an internal field. We carried out this experiment on an Fe-doped crystal to check for such an effect and to see if it also occurred at elevated temperatures.

The experiment was done on a 2-mm-thick crystal of 0.1% Fe-doped $LiNbO_3$. The sample had a cross section of 12 mm (the distance between the c faces) by

9. F. S. Chen, J. Appl. Phys. 40, 3389 (1969).

8 mm. It was mounted on a resistive haater consisting of a thin slab of insulating alumina with a deposited molybdenum heater on the side opposite the sample. The sample was exposed to a 100-mW/cm^2 4880-Å argon laser beam. The resulting photocurrent was measured with a Keithly 610A electrometer set at 10^8-ohm input impedance. This was attached to colloidal graphite contacts on the c faces of the crystal. The contacts were masked so that they were separated from the light by ∿1 mm. Otherwise, the light was incident on the entire cross section of the crystal.

Figure 5 shows the result of a 4-minute exposure at both room temperature and at 200°C. In either case, the light produces (in addition to a sizable pyroelectric effect) a stable photocurrent. This photocurrent always appeared, independent of previous runs, and did not decay even after hours of exposure. Experiments with 1 O.D. neutral density filters showed that the current was proportional to the incident light intensity. It did not appear to depend on the polarization direction of the light.

These results explicitly demonstrate that when Fe-doped $LiNbO_3$ is exposed to light, at room temperature or higher temperatures, a net transport of charge is produced. This transport is most likely the direct cause of hologram storage. The following three points corroborate this assessment.

First, the polarity of the current is consistent with previous hologram storage experiments [10]. From Fig. 5 we see that the current has the same polarity as the pyroelectric current produced by heating. This means that the light produces an internal current (of positive charges) from the +c side of the crystal to the -c side (i.e., in the -c direction). If an external field is applied to oppose this flow (i.e., a field aligned along the +c direction), then the net transport of charge should decrease. If this transport is the origin of the hologram storage, the sensitivity should then decrease. This is indeed what happens. The storage sensitivity decreases upon application of a -c oriented field at both room temperature [2] and at elevated temperatures (Section II).

Second, the higher current at the elevated temperature (see Fig. 5) is accompanied by a similar increase in the sensitivity [2]. The sensitivity increase was not measured for the sample used here but is typically a factor of two or more.

10. D. L. Staebler and J. J. Amodei, J. App. Phys. 43, 1042 (1972).

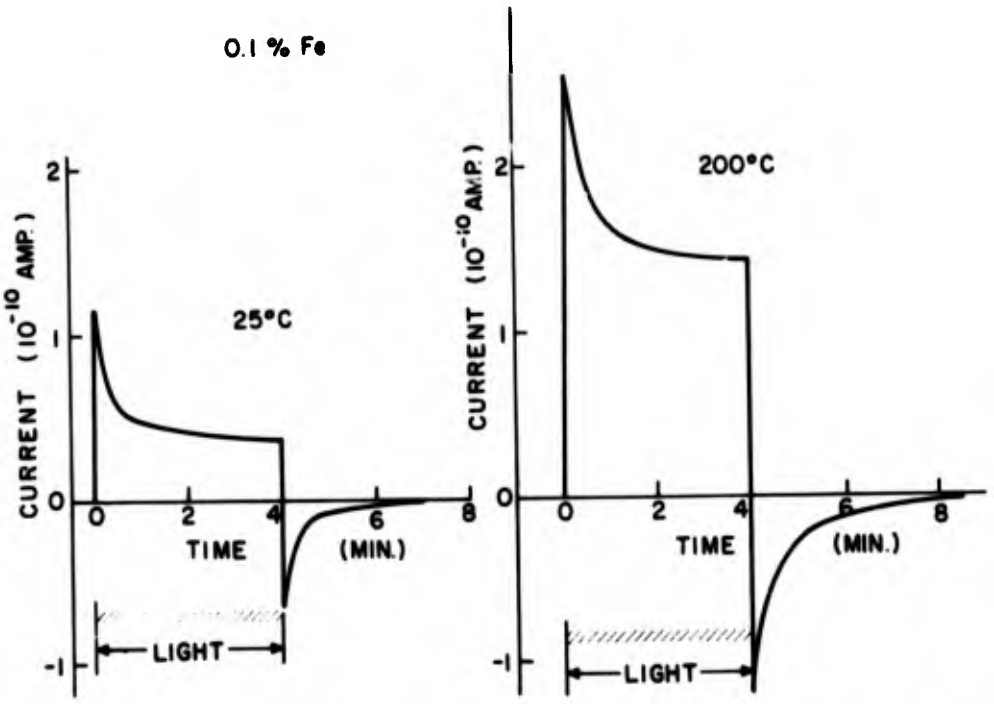

Figure 5. Photoconductivity in Fe-doped $LiNbO_3$. The illumination is 16 mW at 4880 Å argon.

Third, the absolute value of the current agrees with the sensitivity for hologram storage. Previous measurements [7] have shown that, over a wide range of dopings, approximately 1.5 J/cm^2 of absorbed light produce a hologram with 50% diffraction efficiency in Fe-doped $LiNbO_3$. This can be related to the photocurrent shown in Fig. 1 by the following argument. For a 2-mm-thick crystal, a 50% hologram corresponds to a sinusoidal space-charge field ($\Delta E = E_m \cos k x$) of $E_m = 3.5 \times 10^3$ V/cm [11]. It has been shown [10] that this field is related to the current density (j) by

$$\Delta E = -\frac{j}{\varepsilon} t \qquad (4)$$

where t is the time and ε is the dielectric constant. Upon exposure to two equal beams (the conditions for our sensitivity measurements), and assuming a drift model for the storage process, we have

11. J. J. Amodei and D. L. Staebler, RCA Review 33, 71 (1972).

$$j = j_o (1 + \cos k x) \tag{5}$$

Thus we have

$$j_o = \frac{\varepsilon E_m}{t} \tag{6}$$

To relate this to the photocurrent result, we assume an absorbed power density of 75 mW/cm^2, the conditions for the data of Fig. 5, reflections at the front surface of the sample ($\sim$13%), and optical transmission (10%) considered. This intensity requires 20 seconds for a 1.5 J/cm^2 exposure and, from Eq. (6), corresponds to a current density of

$$j_o = \frac{\left[30 \times 8.85 \times 10^{-12}\right]\left[3.5 \times 10^{5}\right]}{20} \ A/m^2 \tag{7}$$

or $j_o = 5 \times 10^{-10}$ A/cm^2. From Eq. (5), we see that this is also the *net* current, i.e., for this experiment k=0. For the cross section of interest (0.2 x 0.8) cm^2, we find a value of $I = 0.8 \times 10^{-10}$ A, in fair agreement with the result shown in Fig. 5 for room temperature.

We can now calculate a mean displacement ($\bar{x}$) of a charge per absorbed photon from

$$j = g \bar{x} e \tag{8}$$

where g is the jump rate and e is the electronic charge. For 75 mW/cm^2 of light absorbed uniformly through the 2-mm thickness of the sample, we have

$$g = \left[\frac{75 \times 10^{-3}}{4 \times 10^{-19}}\right]\left[\frac{1}{0.2}\right] \simeq 9 \times 10^{17} \ \text{jumps/cm}^3 \ \text{s} \tag{9}$$

where we assume unit quantum efficiency; i.e., each absorbed photon produces a jump. Thus we have

$$\bar{x} = \frac{j}{g e} \quad \frac{3 \times 10^{-10}}{\left(9 \times 10^{17}\right)\left(1.6 \times 10^{-19}\right)} \tag{10}$$

or

$$\bar{x} = 2 \times 10^{-9} \ \text{cm} = 0.2 \ \text{Å} \tag{11}$$

as the minimum value for the mean charge displacement per absorbed photon.

B. PHOTOINDUCED COLORATION

Photocolorations consistent with the above results have been produced by exposing a heated crystal of Fe-doped $LiNbO_3$ to a direct laser beam. Figure 6 shows a typical result for a 4-hour exposure of a 2-mm-thick sample of 0.05% Fe-doped $LiNbO_3$. (The sample absorption was $\sim$0.05 O.D.) The sample became clear in the irradiated region, while a dark area forms on the +c side of the clear spot. (The strange central feature was due to the doughnut mode of the laser; i.e., the beam had a hole in it.) A likely model for this effect is that the light excites electrons out of the Fe^{2+} sites (the colored species) and causes them to move in the +c direction. The electrons move until they reach an unilluminated region of the crystal where they are trapped in Fe^{3+} ions to make more Fe^{2+} ions. The net effect is bleaching where the electrons have come from, and coloration where they go. This coloration does not occur at room temperature, because of the strong space-charge fields that are built up. At elevated temperatures, however, these fields are relaxed by ionic conductivity (in the same manner as the fixing process), and the coloration can proceed without interference.

The direction of transport is consistent with the polarity of the photocurrent discussed in subsection A above. The photocurrent was in the -c direction, consistent with negative changes (electrons from Fe^{2+} ions) moving in the +c direction as indicated by Fig. 5.

C. MODEL

A possible model for the above results has been developed. In this model, photoexcitation and subsequent retrapping of electrons on Fe sites shifts the average position of the electrons by an angstrom in the +c direction. The shift occurs in addition to any other transport that the electron undergoes while in the conduction band and, thus, can be formally described as due to drift in an equivalent internal electric field. The magnitude of this equivalent field is simply $(\Delta x/\mu\tau)$ where Δx is the displacement, μ is the mobility, and τ is the lifetime of the free carriers. For heavily doped crystals, rough estimates of μ ($\sim$1 cm^2/V-s) and ($\sim 10^{-12}$ s) lead to an effective field of $\sim 10^4$ V/cm, consistent with the experiment.

Figure 6. Photograph of Fe-doped $LiNbO_3$ after extended exposure to 4880 Å argon laser beam. The dark coloration is on the +c side of the illuminated region.

The unidirectional transport may be qualitatively understood by the following argument. We identify the Fe^{2+} absorption band as due to the transition of an electron from an Fe^{2+} ion (substitutionally occupying a Li^{+} site) to the d orbital of a nearby Nb^{5+} ion. The conduction band is derived from d orbitals on the Nb ion. This transition probability depends upon the overlap between the Fe^{2+} and Nb^{5+} wave functions. The closest Nb^{5+} ion to the substitutional Fe^{2+} is along the +c axis, resulting in a higher probability of excitation in this direction [12].

12. M. G. Clark, F. J. DiSalvo, A. M. Glass, and G. E. Peterson, J. Chem. Phys. 59, 6209 (1973).

As described above, this unidirectional transport is formally equivalent to an internal field. Although a uniform electric field actually is not present, this description is useful to explain the erase/record behavior of the crystals and how it varies with doping level. The application of this model to the erase/record asymmetry will be discussed in Section V.

In order to not "undo" the unidirectional excitation with a unidirectional recombination in the opposite direction, we assume the lattice polarization around the Fe^{3+} sites is such that the recombination probability is more symmetric along the c axis than is the excitation. Such a model has also been proposed by Clark et al. [12].

SECTION IV

IDENTIFICATION OF THE MOBILE IONIC SPECIES

A key element in the storage of fixed holograms in $LiNbO_3$ has been the presence of an unknown ionic species which is mobile at a temperature of 160°C [2]. In Section II we determined the activation energy for their motion in Fe-doped $LiNbO_3$. The transport behavior of these ions is extremely important since thermal erasure of the holograms takes place while the ions are moving to fix the holograms. The relative rates of hologram fixing and erasure determine the number and diffraction efficiency of the final fixed holograms. Until now, there has been no identification of this/these species. In this section we present results of experiments designed to identify the mobile ions.

In Section III of this report, we showed that the unidirectional transport of electrons in the absence of a field could take place over very large distances in Fe-doped $LiNbO_3$. As can be seen from Fig. 6, electrons excited from Fe^{2+} ions moved out of the illuminated region and stopped their transport at the edge of the light spot. This resulted in the bleaching of the illuminated region and the dark coloration at the +c edge of the illuminated spot. If the experiment is done with the sample hot, the mobile ionic species can follow the transport of the electrons and there will be no net space charge built up. If the experiment is performed with the sample at room temperature, there is no observable change in the coloration, presumably because a small amount of unscreened electron transport takes place which establishes a field in opposition to the electrons' preference to move in the +c direction.

It was shown in Section II that the field which "neutralizes" the preferential transport is on the order of 10^4 V/cm. Such a field will be produced by a surface charge of 10^{11} electrons/cm^2 in $LiNbO_3$. A shift of this small number of electrons to the edge of the spot, which will then result in no further transport, will not result in a significant optical change. Because we observe the bleaching when the sample is hot, the ions must have moved to screen the electronic charge. Therefore, there is a high concentration of the mobile ionic species in the same region where there is a high concentration of the electrons.

In order to identify the mobile ions which move to screen the transported electron charge, a number of different crystals and dopant levels were studied.* In each case the +c face of the crystals were polished to a window glass finish prior to laser irradiation. This was found to be necessary to reduce the noise level on the X-ray emission from the crystal. The crystals were then heated to ∿200°C and irradiated with a 4880 Å laser beam (∿3 w/cm^2) for several hours. An electron microprobe beam was then scanned along the +c face as shown schematically in Fig. 7. The microprobe hits the surface with a small electron beam (∿2 μm in diameter, 25 kV, 0.1 μA) which excites X-ray transitions in atoms within ∿1 μm of the surface. The emitted X-rays are then analyzed in an X-ray spectrometer. Well-known characteristic emission lines of the different elements are then correlated with the observed emission spectrum. This technique is sensitive to concentration changes on the order of 0.01% by weight.

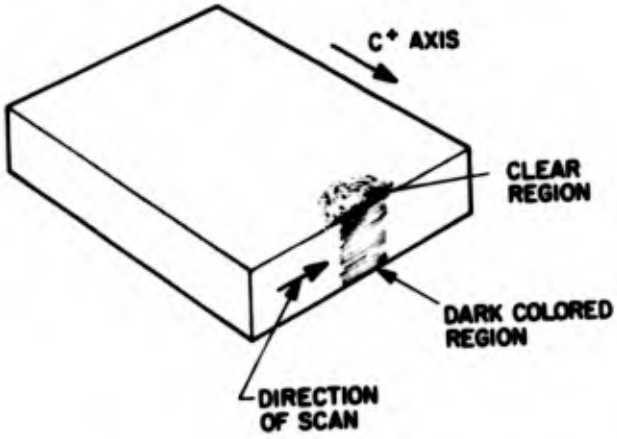

Figure 7. Schematic drawing of configuration for electrom microprobe experiment.

A number of scans were then made on different crystals to obtain the magnitude and spatial distribution of the mobile species. Crystals containing 0.05%, 0.5%, and 1% by weight of Fe were studied. Clear indications of the

*The laser light spot illuminated a region which included a +c face. It was intended to cause the electrons and ions to transport to the surface where the ions could be found by the electron microprobe.

presence of an excess concentration of Si were observed in several different samples, containing 0.5 or 1% Fe. Si present on the surface of the 0.05% sample could not be detected presumably because the concentration of Fe traps and thus of compensating ions was too small. Figure 8(a) shows a photograph of one such sample containing 0.5% Fe; Fig. 8(b) is a schematic drawing of the same crystal. The dark coloration at the edge of the sample is due to the high concentration of electrons at the surface. The dark spots in the bleached region are due to small regions of reversed domains where the electrons have transported in the +c direction within their own domain. These dark spots appear as comet-like objects with their heads pointed in the -c direction when viewed in the microscope. These domains are clearly bulk effects since one has to focus down from the crystal surface to observe them. They are quite distinct from effects observed around cracks in the crystal surface or edges.

The trace from a microprobe scan along the +c face is shown in Fig. 9. Notice that the Nb line is flat within the experimental noise. This is to be expected. Under our assumptions, the electrons occupy Fe sites converting Fe^{3+} centers into colored Fe^{2+} centers. The excess concentration of electrons at the surface (and, hence, the excess concentration of mobile ions) should be no greater than the number of Fe^{3+} sites available. Because the Fe-doping level is 0.5%, changes in the Nb concentration, if it were the mobile species, would be only on this order. Fractional changes of that magnitude are unobservable by this technique. However, the concentration of Fe or of any other trace impurity element should be significantly affected. Notice that the Fe trace shows no change when the beam is scanned across the darkened area. However, there is a significant increase in the Si trace.

In the course of examining several other crystals which confirmed these results, we found another sample containing 0.5% Fe which has a nonuniform coloration on the c face after laser irradiation at 200°C. A photograph of a portion of the c face taken at 60X is shown in Fig. 10(a) and schematically in Fig. 10(b). The dark areas are observed as having a deep cherry red color which is indicative of a large local concentration of Fe^{2+}. The patchy appearance of this sample probably originates from the fact that it is not fully poled in this region and has multiple domain structure. The positive domains become darkly colored whereas the negative domains become lighter, leading to the observed patches. Figures 11 and 12 show the results of

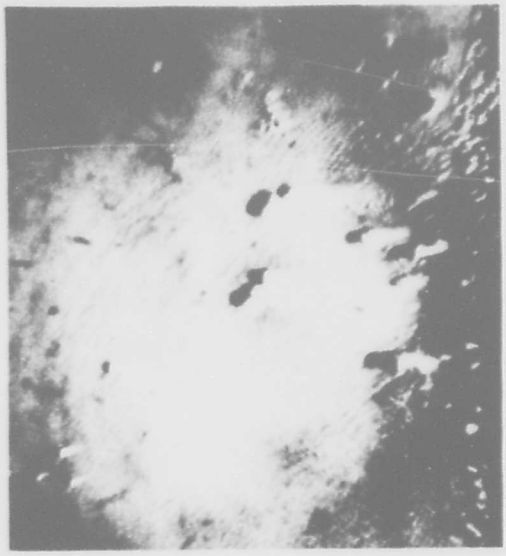

(a)

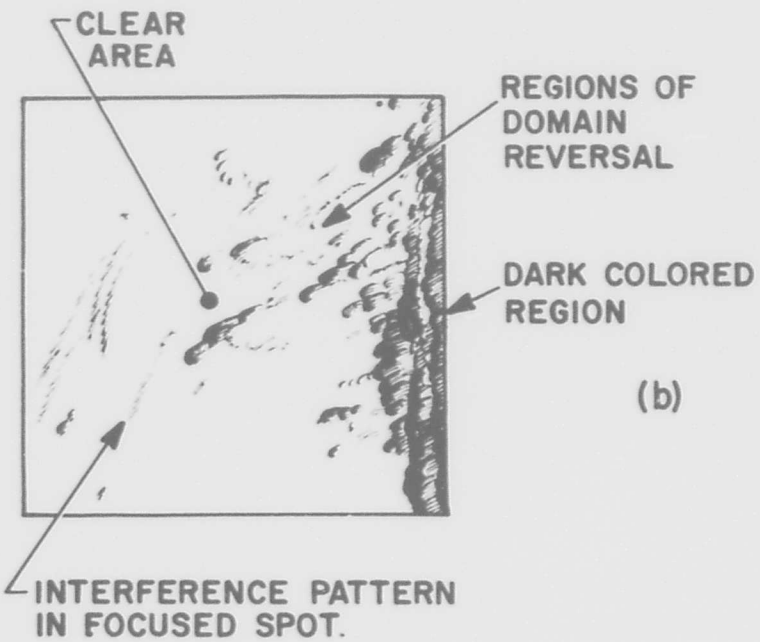

Figure 8. (a) Photograph of a sample as in Fig. 6 where the exposure is at the crystal +c edge and (b) schematic drawing of crystal shown in Fig. 8(a).

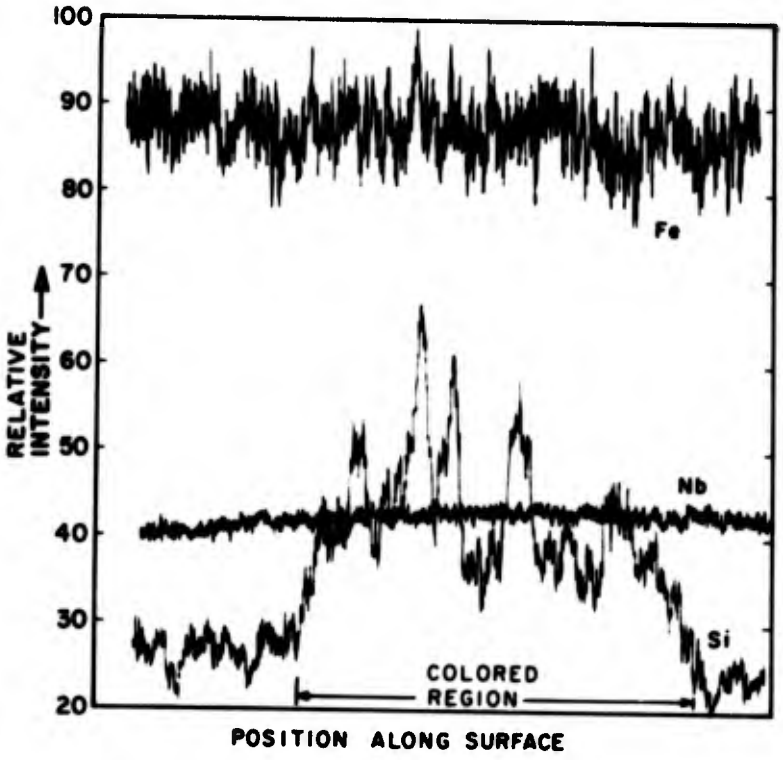

Figure 9. Tracings of electron microprobe scan for Nb, Fe, and Si.

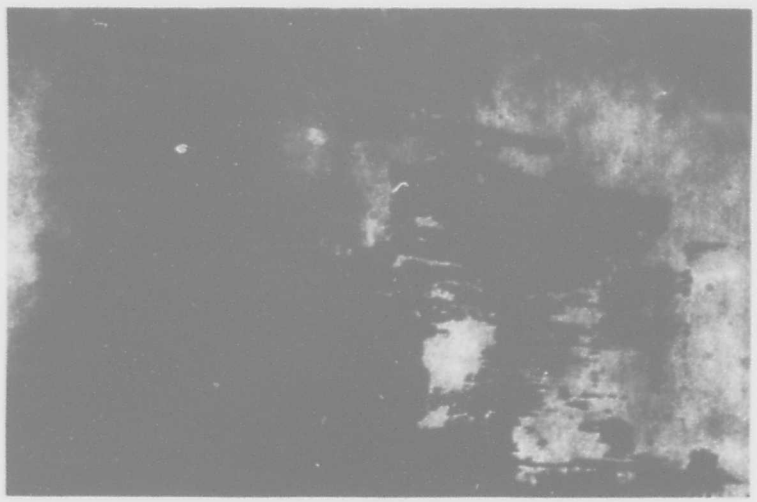

(a)

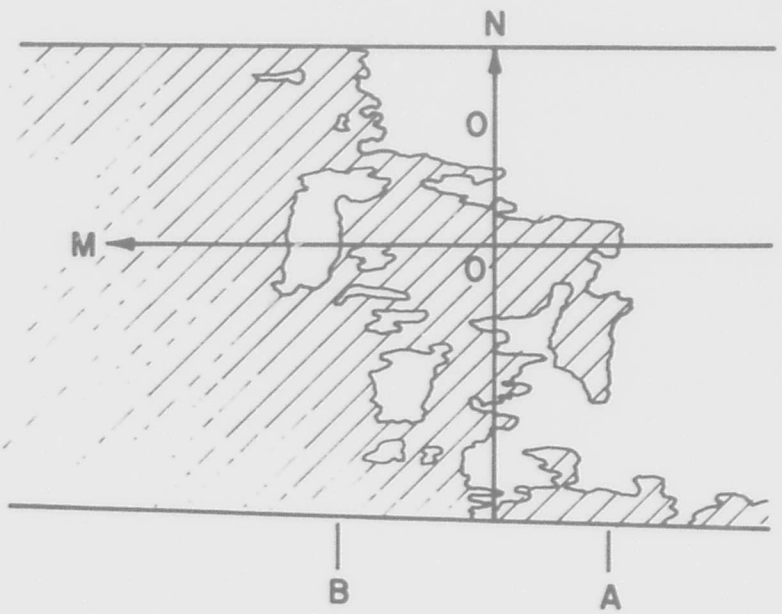

(b)

Figure 10. (a) Photograph of +c face of 0.5% Fe-doped $LiNbO_3$ crystal. The dark coloration is due to a heavy concentration of Fe^{2+}.
(b) Schematic drawing of crystal in (a). Lines labelled M and N are microprobe scan lines. Circles show areas where qualitative analysis was done.

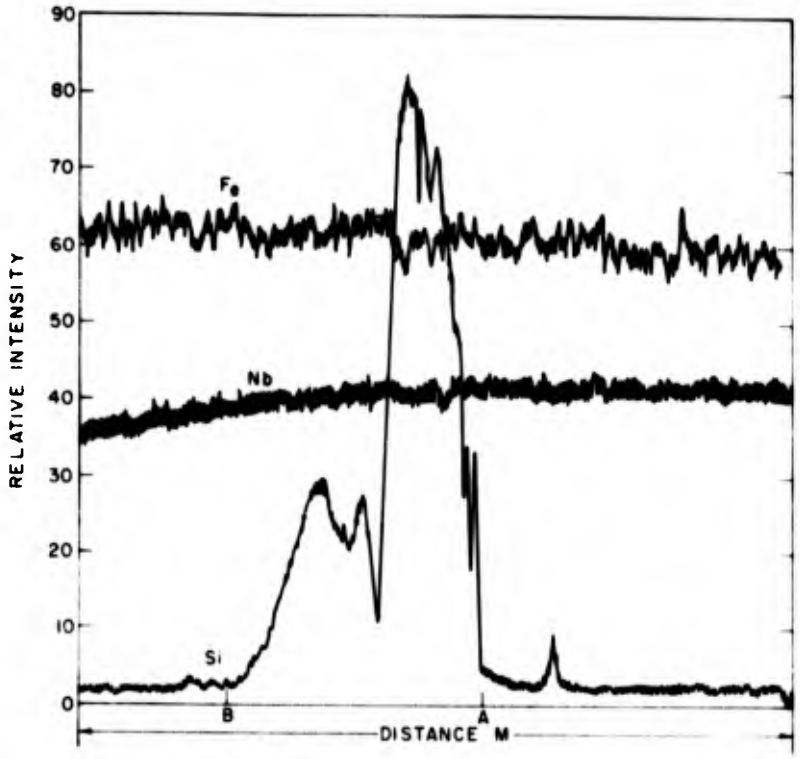

Figure 11. Tracing of electron microprobe scans for Nb, Fe, and Si along line M shown schematically in Fig. 10(b).

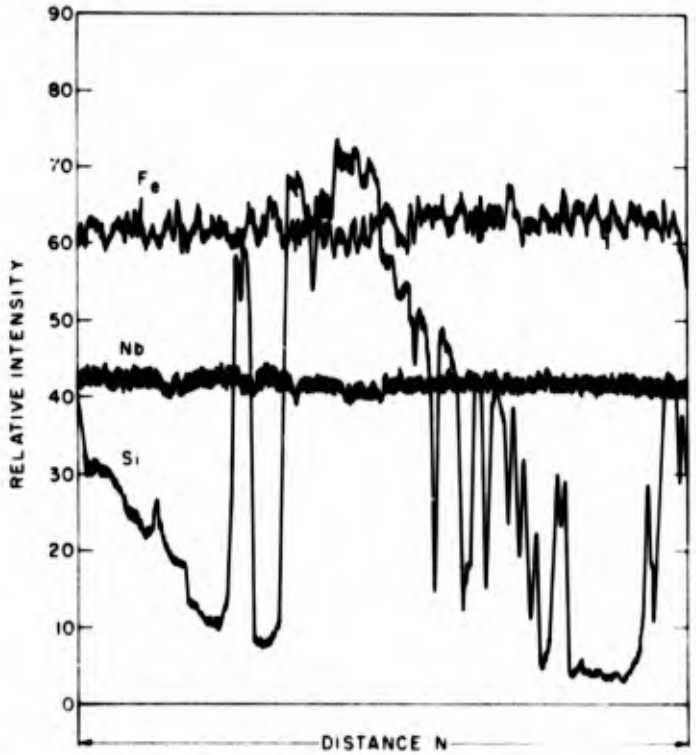

Figure 12. Tracing of electron microprobe scans for Nb, Fe, and Si along line N shown schematically in Fig. 10(b).

microprobe scans along the lines M and N as drawn in Fig. 10(b), respectively, in the directions indicated. These results along the line M have excellent signal-to-noise and show strong Si X-ray emission which can be correlated with the visually observed dark patches. The data taken on the N line give results similar to those for the M line. It is interesting to note the large increase in Si X-ray emission near the edges of the face. We believe this increase to be real but cannot at present account for it.

The excess surface concentration of Si most probably moves to the surface from the bulk of the sample. To search for a variation in Si concentration, the sample shown in Fig. 10(a) and 10(b) was cut parallel to the line N and the polished down to this line. A microprobe scan along this surface parallel to the c-axis showed no significant variation in intensity. This is most probably due to the fact that the layer of Si ions on the surface is significantly smaller than the spatial resolution of this technique. The X-ray emission from the surface is collected from an area 3 to 4 μm in diameter even though the electron beam is only 1 μm in diameter.

Fe-doped $LiNbO_3$ contains a number of different impurities which are present in trace concentrations:

Al	15 to 150 ppm
Cu	0.1 to 1 ppm
Mg	5 to 50 ppm
Mn	3 to 30 ppm
Si	3 to 30 ppm

Qualitative analysis was made in the regions circled in Fig. 10(b). This work showed that for $N \geq 13$ (Al), only Si was present in an excess concentration sufficient to be detected by the microprobe. This indicates then that Al, Mg, Mn are not ionic compensators in this material at temperatures less than 200°C.

The results presented above indicate that Si is the only trace impurity element with an atomic number greater than 13 (Al) which contributes significantly to the fixing of holograms in crystals of Fe-doped $LiNbO_3$. The microprobe technique does not rule out the possibility that interstitial Li or Nb or O vacancies (which would also move to the surface) contribute since small changes in the surface concentrations of the interstitials could not be detected while O vacancies cannot be detected by this technique. These experiments,

then, do not rule out the possibility that either one of the above species, or elements with N ≤ 13, is the dominant mobile species and that the Si, while it is mobile, is not the dominant ionic compensator. In the analysis which follows we shall *assume* that the 1.18-eV activation energy which we observe is the activation energy for Si motion and that the Si ion is the only mobile ionic species.

Si^{+4} is the most common ionization state of this ion. We know that the compensating silicon ions represent positive charge in the lattice since they screen the electrons. Thus the Si ion cannot sit on a Nb^{5+} lattice site since it would be negatively charged. This ion could sit on the Li site since it would have a net positive charge relative to the lattice. Since its radius (0.41 Å) is less than that of the Li^{+} ion (0.6 Å), it can fit into that site. An alternative possibility is that the Si^{+4} ion exists as an interstitial. A large interstitial void exists along the c-axis alternating with Li-Nb pairs.

Since the conductivity and activation energy for the mobile ions have been measured previously and from the results and model presented above we can determine a concentration and charge for the mobile ion, the motion of the ion can be analyzed. The following quantities are known:

The conductivity σ_i	$= 2 \times 10^{-13}$ mho/cm @ T = 160°C
The mobile ion concentration n_i	$\approx 1.9 \times 10^{17}$ Si ions/cm^3 = 10 ppm
The activation energy ε_a	= 1.18 eV
The ionic charge q	$= 4\ e = 6.4 \times 10^{-19}$ coul

The ionic conductivity is described as a hopping process between sites where the Si ion can sit and can be described by [13]:

$$\sigma_i = n_i q \mu_i = \frac{n_i q^2 \nu a^2}{kT} e^{-\varepsilon_a/kT} \qquad (12)$$

where ν is the vibrational frequency of an ion in its potential well and a is the jump length for the mobile ion. In Eq. (12) the anisotropy in ν and the variation in barrier height with temperature have been neglected.

The ionic mobility μ_i is:

$$\mu_i = \frac{q \nu a^2}{kT} e^{-\varepsilon_a/kT} \qquad (13)$$

13. N. F. Mott and R. W. Gurney "Electronic Processes In Ionic Crystals," (Oxford University Press, London, 1951), p. 26.

Using Eq. (12), the mobility at 160°C is

$$\mu_i = \frac{\sigma_i}{n_i q} = 1.6 \times 10^{-12} \frac{cm^2}{volt\text{-}s} \tag{14}$$

Using Eqs. (13) and (14) the jump length is:

$$a = \left\{\left(\frac{kT}{q}\right) \frac{\mu}{\nu e^{-\varepsilon_a/kT}}\right\}^{1/2} = 50\ \text{Å} \tag{15}$$

for $\nu = 10^{13}$ Hz. This corresponds to a jump of approximately three unit cells along the c-axis in $LiNbO_3$. Using the Einstein relation and Eq. (13), the diffusion coefficient is

$$D = \frac{kT\mu}{q} = \nu a^2 e^{-\varepsilon_a/kT} = 1.5 \times 10^{-14}\ cm^2/s \tag{16}$$

Eq. (16) can also be written in the form

$$D = D_o e^{-\varepsilon_a/kT} \qquad \text{where } D_o = 2.4 \tag{17}$$

using $\varepsilon_a = 1.18$ eV and T = 160°C. This value of D_o is remarkably large, comparable to the diffusion constant of Li in Ge. In that case, the Ge crystals must be kept cold to prevent redistribution of the Li which would take place at room temperature. Because of the large D, it seems the Si diffusion in $LiNbO_3$ may take place along large interstitial channels which exist in this crystal structure. This large diffusion constant is worthy of further investigation.

Holograms are recorded in Fe-doped $LiNbO_3$ at a temperature of 160°C since at this temperature ionic compensation occurs at essentially the same rate as the electronic space-charge pattern is formed. Lower temperatures and thus slower compensation rates allow buildup of electric fields which in turn leads to spurious optical scattering that degrades image quality. At higher temperatures increased thermal erasure leads to lower diffraction-efficiency fixed holograms. At 160°C optical and thermal erasure are comparable in magnitude. The efficiency of holographic storage will be improved if the ionic conductivity can be increased since the recording temperature and thus the thermal erasure can be decreased.

From our previous work [3] we know that the ionic conductivity at T = 160°C is sufficient to provide fast compensation of an electronic space-charge pattern. From Eq. (12) it is clear that if the concentration of mo mobile ions n_i is increased, then the required operating temperature can be reduced. Alternatively one can ask how much must the concentration of mobile ions be increased to lower the operating temperature by a given amount. Using Eq. (12) the concentration of mobile ions must be increased by a factor of 4.9 (to $9 \times 10^{17}/cm^3$) to reduce the operating temperature from 160°C to 140°C, while maintaining the fixing rate at the same level. We now consider the effect of this lower temperature on the thermal excitation of the electrons.

The thermal erasure rate R is

$$R = g\, e^{-\varepsilon/kT} \tag{18}$$

where g is a constant and $\varepsilon = 1.48$ eV is the electron activation energy for thermal ionization of filled traps. A reduction of the operating temperature from 160° to 140°C produces a reduction of a factor of 7.3 in the rate of thermal erasure. Such a decrease, if obtained, would make the thermal erasure negligible in comparison with the optical erasure. This leads to approximately a factor of two increases in the erase/record asymmetry β.

We have observed variations of a factor of two to four in the ionic relaxation in Fe- and Mn-doped samples which may be attributable to as-grown variations in the Si-concentration.

The relationship between β, the number of holograms recorded N, and the diffraction efficiencies of the first (η_o) and last (η_N) holograms recorded is:

$$N = 1 + \beta \left(\frac{\eta_o}{\eta_N} - 1 \right)^{1/2} \tag{19}$$

It is clear from this equation that, for $\beta >> 1$, doubling the asymmetry β allows twice the number of holograms to be recorded with the same final diffraction efficiency η_N. Alternatively, if the same number of holograms are

recorded, the diffraction efficiency of the final hologram can be greater assuming the diffraction efficiency of the first hologram is the same in both cases. Using Eq. (19)

$$\frac{\eta_o'}{\eta_n'} = 1 + \frac{\beta^2}{\beta'^2}\frac{\eta_o}{\eta_N} - 1 \tag{20}$$

where the primed quantities refer to the case where the asymmetry has been doubled (i.e., $\beta' = 2\beta$). At present for N = 500 holograms, $\eta_o = 0.5$ and $\eta_N = 0.03$ (see Section I) are typically used. If $\eta_o' = \eta_o$ then the efficiency of the last hologram recorded is:

$$\eta_N' = 0.15$$

If $\eta_N' = \eta_N = 0.03$, then the first hologram recorded need have only a diffraction efficiency $\eta_o' = 0.15$.

From this calculation we see that a doubling of the asymmetry leads to significantly improved performance. In particular at the present storage capacity of 500 holograms, a factor of five increase in the diffraction efficiency per hologram should be obtainable, or for 3% diffraction efficiency holograms the recording time at the same exposure is reduced by approximately a factor of two.

The model presented in Section V shows that a similar increase in asymmetry can be obtained by increasing the Fe^{3+} concentration. This process would appear to be a simpler approach but it is not an unlimited one since a uniform, small, fixed concentration of Fe^{2+} ions can be obtained only with great difficulty, if at all, in thick, very heavily doped crystals. In addition, the increase in the empty trap concentration decreases the optical erasure. From a practical point of view certain amounts of optical erasure is desirable in $LiNbO_3$ in order to erase any spurious optical damage occurring during readout.

SECTION V

MULTIPLE STORAGE

Multiple storage in $LiNbO_3$ proceeds by the sequential storage of holograms. As discussed in previous reports, the recording of a hologram partially erases those holograms stored previously. At room temperature, erasure occurs via the same mechanism as recording: optical excitation of a trapped electron into the conduction band and subsequent retrapping. At the higher temperatures ($\sim$160°C) used with the record-while-hot technique, erasure can also occur via thermal ionization of a trapped electron and subsequent retrapping. The dynamics of this process are discussed in Section II of this report. At high temperatures, the erasure is a sum of optical and thermal processes.

The key to improved multiple storage in Fe-doped $LiNbO_3$ is to increase the ratio of the characteristic erasure to writing times. In our previous work [3], this ratio was approximately 15, which enabled us to record up to 100 holograms with diffraction efficiencies of 1%.

We have recently obtained new crystals of Fe-doped $LiNbO_3$ which have enabled us to record over 500 holograms with diffraction efficiencies per hologram ranging from 2.5 to 25% in a single recording. The results obtained to date with these new crystals and the implications of these results for multiple storage are discussed below.

A. SAMPLE PREPARATION

Crystals to be used for multiple storage experiments have to meet three requirements:

(1) They have to be thick, on the order of 1 cm, to obtain the desired small angular separation between holograms.

(2) The optical density has to be in the neighborhood of 0.3 (1/2 the light absorbed) to maximize the overall record-readout efficiency.

(3) The Fe^{2+} concentration has to be uniform throughout the thickness of the crystal.

To prepare these crystals, we made use of the technique developed under a previous phase of the program [2]. The crystals were annealed at a constant, resettable temperature in a mixture of argon and oxygen. This was done for a sufficiently long time to ensure that the Fe^{2+} concentration reached a steady state. Then they were cooled at a low but repeatable rate to room temperature. The desired degree of reduction of the crystals was achieved by adjusting the argon-oxygen mixture on an empirical basis.

This procedure makes use of the fact that, at a given temperature, the Fe^{2+}-to-Fe^{3+} ratio in a crystal will reach an equilibrium value determined by the overall Fe concentration in the crystal and the oxygen partial-pressure in the ambient atmosphere. However, when the crystals are cooled slowly, there is a tendency for the Fe^{2+} concentration to decrease as the temperature falls. The kinetics of this decrease eventually become too slow to follow the temperature. Therefore, the cooling rate can be set sufficiently low that large crystals can follow it uniformly, yet some of the Fe^{2+} concentration induced at the anneal temperature will persist during the cooling.

During the contract period, we accomplished two things in this area: (1) tested the repeatability of the procedure outlined above and (2) built up a set of empirical data that would allow us to color crystals on a routine basis for multiple storage experiments. We used a tube furnace which could be set for 975°C and programmed downward at 100°C per hour. Gas was supplied from premixed, high-purity argon-oxygen mixtures containing 0.2% O_2, 1% O_2, or 10% O_2. Other mixtures could be obtained using a high-precision dual flow meter by mixing the premixed gas with pure argon.

Figure 13 summarizes data obtained for various samples from three different crystals. The procedure demonstrates a strong measure of predictability. This preparation procedure and the data of Fig. 13 were used to prepare the new crystals described below.

The results discussed here were obtained using a boule of Fe-doped $LiNbO_3$, containing 0.02 mole % Fe, which was grown by the Crystal Technology Corporation. With the exception of an increased storage capacity, crystals cut from this boule behaved essentially identically with crystals studied previously in terms of their optical absorption, recording sensitivity, behavior under oxidation-reduction treatment, and in their ionic conductivity (see Section II). A boule containing 0.005 mole % Fe grown at the same time

behaved identically under these same treatments when allowance was made for the different dopant concentration. The erase/write asymmetry of crystals cut from this boule was much smaller than those obtained from the 0.02 mole % Fe-doped boule, and, therefore, they were not studied extensively. This result is consistent with our overall understanding of the recording process and the specific results of subsection C below.

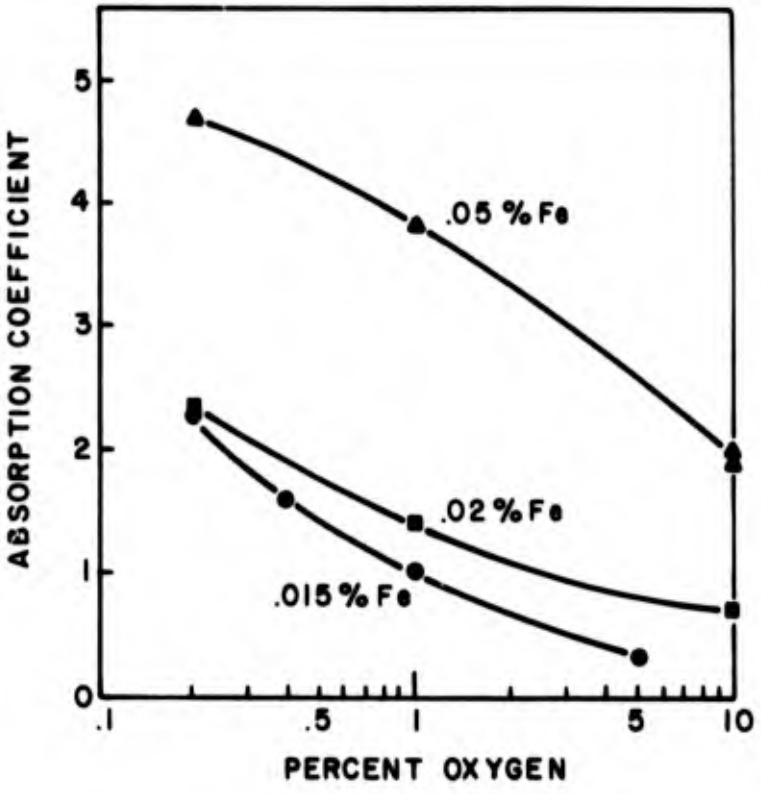

Figure 13. Absorption coefficient produced in Fe-doped $LiNbO_3$ crystals as a function of the oxygen content of this argon-oxygen reducing atmosphere.

B. MULTIPLE STORAGE AND ASYMMETRY

Using crystals cut from the 0.02 mole % Fe-doped $LiNbO_3$ boule, we have carried out several experiments to determine the erase/record asymmetry and the number of holograms and the diffraction efficiency per hologram obtainable in these crystals. Crystals with thicknesses ranging from 0.5 to 1.0 cm were colored uniformly to an optical density of 0.3 at 4880 Å using the techniques discussed above. Holograms were then recorded at room temperature and 160°C,

mechanically stepping the angle from one value to another. The holograms were spaced 0.10° apart. The asymmetry was measured by recording 40 to 100 holograms, each with the same exposure. The results of such a measurement on a 1-cm-thick crystal are shown in Fig. 14. To determine the asymmetry ratio β we use the relation

$$\beta = (n - 1)\left\{\frac{\eta_1}{\eta_n} - 1\right\}^{-1/2} \tag{21}$$

where n is the number of holograms recorded, and η_1 and η_n are the efficiencies of the first and n^{th} holograms recorded. An asymmetry $\beta \tilde{\sim} 75$ is obtained from the data shown in Fig. 14.

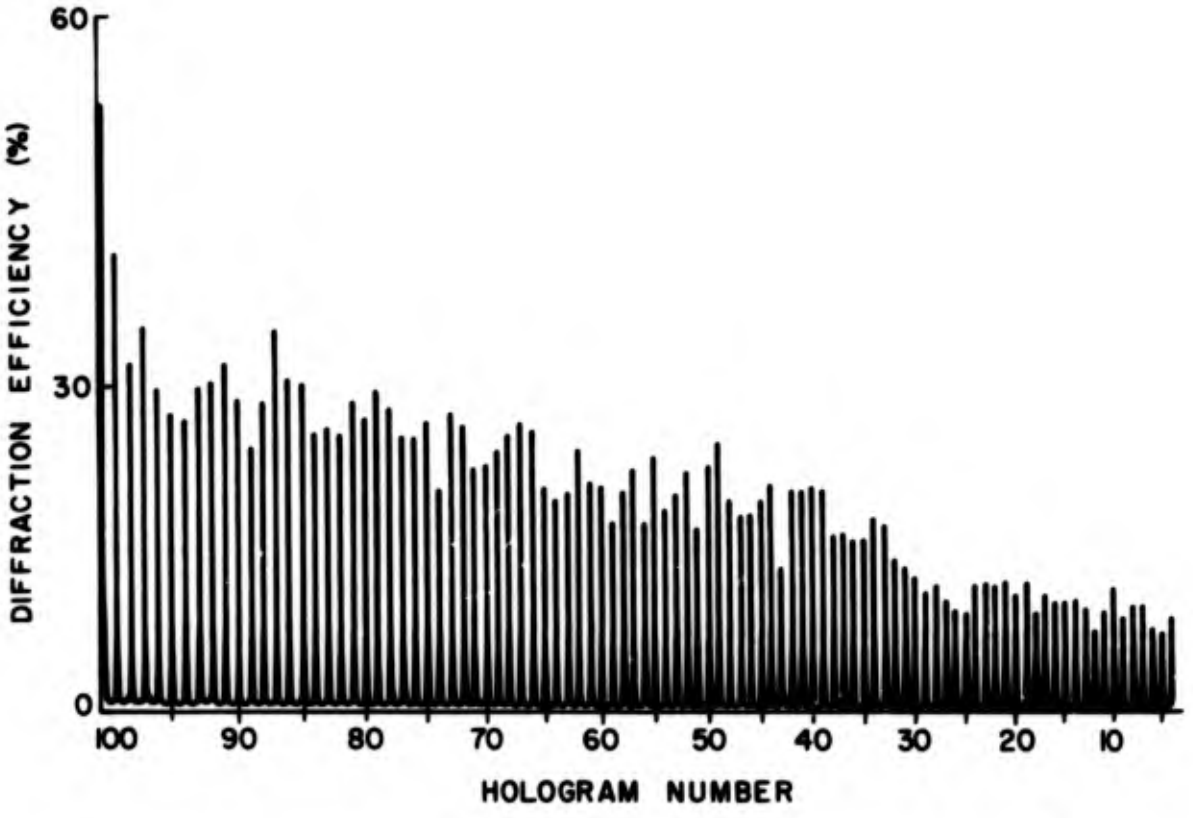

Figure 14. Readout of 100 fixed holograms recorded with constant exposure time. The rolloff in diffraction efficiency is a measure of the erase/write asymmetry.

Using this value for the asymmetry, we control the exposure during writing so that on readout, all the holograms will have the same efficiencies. More than 200 holograms were recorded in a 0.5-cm-thick crystal with diffraction efficiencies uniformly decreasing from 40% for the first hologram recorded to 4% for the last one recorded. In a 1.0-cm-thick crystal, more than 500 holograms were recorded with diffraction efficiencies uniformly decreasing from 25% for the first hologram recorded to 2.5% for the last one recorded. In these tests the recording time per hologram was decreased in successive holograms, as discussed in an earlier report [1], in order to compensate for the optical and thermal erasure. Invariably the results obtained were as cited above: not as much erasure of the first hologram as was expected. This is due, we believe, to an underestimate of the erase/write asymmetry obtained from the constant exposure/hologram studies discussed above. Since uniformity of diffraction efficiency is not an important problem at this time, no effort was made to rerecord with a different value of the asymmetry. The fact that the results obtained indicate that we are, in fact, still underestimating the asymmetry makes these observations even more remarkable.

C. THEORY

As noted in the introduction to this section, the key to improved performance of Fe-doped $LiNbO_3$ lies in improving the erase/record asymmetry which is the *ratio* of the characteristic erasure to writing times. Here we present explicit expressions for this ratio to examine its dependence on doping levels. The asymmetry at both room temperature and 160°C are given for the case of Fe-doped crystals where the recording is assisted by an internal field.

We shall first calculate the time T_R required to produce an electronic space-charge field of magnitude E_{sc} at either 22° or 160°C. We shall then calculate the time constant T_E for optical erasure at room temperature and the time constant T_E' for optical and thermal erasure at 160°C. The erase/record asymmetry at 22°C is then

$$\beta = T_E/T_R \tag{22}$$

and at 160°C the asymmetry is

$$\beta = T_E'/T_R \tag{23}$$

At both 22°C and 160°C the recording process behaves as though an internal field were present in the crystal. To calculate the recording time we use Section III of this report where it was shown that this apparent internal field arose from the net translation along the +c axis that occurs on generation of free electrons. Diffusion of the free electrons which occurs during the recording of the hologram is not important since it is a symmetric process while the electric field produced is not symmetric but is equivalent to a translation of charge in the +c direction only. The current produced by the translation process is

$$J = \bar{x}e \frac{I_o N\sigma}{h\nu} (1 + m \cos Kx) = \bar{x}eNg_R (1 + m \cos Kx) \tag{24}$$

where I_o is the incident power at frequency ν, $\bar{x}$ is the net translation per excitation, N is the trapped charge concentration, σ is the absorption cross section, and g_R is then $I_o\sigma/h\nu$, the generation rate per trap. The buildup in charge density is then

$$\rho(x) = - \int_o^t \frac{dJ}{dx} dt = \underline{\bar{x}eNtg_R} \, mK \sin Kx \tag{25}$$

The resulting electric space-charge field is

$$E_{sc} = \int \frac{\rho}{\epsilon} dx = - \frac{\bar{x}eNmt}{\epsilon} \cos Kx \tag{26}$$

The time T_R to record a space-charge field E_{sc} is:

$$T_R = \frac{\epsilon E_{sc}}{\epsilon \, eg_R mN} \cdot \frac{1}{\bar{x}} \tag{27}$$

The erasure process involves optically and thermally generated photoelectrons which drift in the recorded space-charge field in crystals at room temperature and diffuse along the charge density gradient of the compensated electronic space-charge distribution at higher temperatures. The generation rate per trap g is constant throughout the crystal since the erasing optical

beam and the temperature are uniform. The number of free electrons n generated is

$$n \sim \left\{ N - \frac{\rho(x)}{e} \right\} g\tau \tag{28}$$

where $\rho(x)$ is the spatially varying charge density of the recorded grating. $n << N$ is always true in the case of Fe-doped $LiNbO_3$ crystals.

At room temperature, erasure with a uniform beam proceeds via drift in the space-charge field of the grating. Amodei [14] has shown that the characteristic time T_E for this process is:

$$T_E = \frac{\varepsilon}{Ne\mu g_E \tau} \tag{29}$$

where g_E is optical generation rate of electrons during erasure at room temperature and τ is the electron lifetime.

At T = 160°C erasure proceeds via diffusion since the space-charge field is compensated by ionic motion. For this case the characteristic erasure time T_E' as derived in Section II above is:

$$T_E' = \frac{1}{Dg_E' \tau K^2} \tag{30}$$

where $D = kT\mu/e$ is the diffusion constant, K is the grating constant, g_E' is the generation rate per trap at T = 160°C and has both thermal and optical components during erasure, and τ is the lifetime of an electron at 160°C.

Using Eqs. (27) and (29) the asymmetry ratio at room temperature is:

$$\beta = \frac{T_E}{T_R} = \frac{\bar{mx}}{E_{sc}\mu\tau} \tag{31}$$

Using Eqs. (27) and (30) the asymmetry ratio at high temperatures is:

$$\beta' = \frac{T_E'}{T_R} = \left(\frac{eN}{\varepsilon DK^2} \right) \left(\frac{\bar{mx}}{E_{sc}\tau} \right) \left(\frac{g_R}{g_E'} \right) \tag{32}$$

14. J. J. Amodei, RCA Review 32, 185 (1971).

Except for the thermal effects, $g_E' = g_R$. Then the difference between Eqs. (31) and (32) is a factor ($\mu eN/eDK^2$) where we have multiplied Eq. (32) by μ/μ for purposes of comparison. Assuming $N = 10^{16}/cm^3$, $m = 1$, $\ell = 10^{-4}$ cm, and $\mu \gtrsim 1$ cm^2/V-s, the quantity

$$\frac{\mu eN}{\epsilon DK^2} \gtrsim 1 \tag{33}$$

i.e., the asymmetries are of the same magnitude when the additional thermal erasure at high temperatures is accounted for. This is consistent with our experimental results.

We now consider the effect of doping on β. The experimental observation is that for constant optical absorption the asymmetry increases with Fe concentration since the concentration of Fe^{2+} in crystals of a given thickness remains fixed to give a $\sim$50% absorption of the recording and readout light. To relate β to the trap concentration we use the dependence of the lifetime on the trap concentration. The electronic lifetime τ is:

$$\tau = \frac{1}{pvs} \tag{34}$$

where p is the empty trap density, v is the thermal velocity in the conduction band, and s is the cross section for electron trapping by the Fe^{3+} ion. Substituting Eq. (34) into Eq. (31) or (32)

$$\beta = \text{const} \times p \tag{35}$$

The asymmetry is then a linear function of the empty trap density for the case where the recording process is dominated by the effective internal field.

The cross-over from a recording process dominated by diffusion to one dominated by a drift-like process takes place when the diffusion velocity, DK, is equal to the drift velocity, $\bar{x}/\tau$. Using Eq. (34), the empty trap concentration at which the cross-over occurs at room temperature is:

$$p = \frac{DK}{vs\bar{x}} = 1.5 \times 10^{18}\ Fe^{3+}/cm^3 \tag{36}$$

where $K = 2\pi/\ell$, $\ell = 10^{-4}$ cm, $v = 10^7$ cm/s, $s = 10^{-14}$ cm^2 and $\bar{x} = 10^{-8}$ cm.

This value corresponds to a total Fe concentration of ≈0.01%. This agrees well with our findings that the drift effect begins to dominate in the range of 0.005%.

This result shows clearly that large gains in the erase/record asymmetry in Fe-doped $LiNbO_3$ are possible. In Section III above we discussed the effect of a factor of two increase in the asymmetry. A large increase is clearly possible by simply increasing the Fe doping level. The obtainable increase will be limited, however, by the difficulty encountered in obtaining the required small, uniform concentration of Fe^{2+} in very heavily doped crystals.

D. DEVICE IMPLICATIONS

The results presented above show that the storage capacity of 1000 holograms stored in one crystal can be met with Fe-doped $LiNbO_3$. In addition, the high diffraction efficiency (∿10%) that can be achieved with these materials is important in that lower power lasers can be used on readout, thus reducing the magnitude of the optically induced scattering as well as reducing the overall system cost, size, and complexity. Further improvements may be possible through further increases in Fe doping and by reduction of thermal erasure through increased ionic conductivity.

The image quality obtained at the level of 500 holograms recorded and fixed can be described as poor to good. With proper angular separation (7 to 9 holograms per degree) cross talk between holograms can be reduced to acceptable levels. The major contributions to the noise in the readout image were due to physical imperfections in the optical system, multiple reflections which give rise to interference fringes in the image, and recording beam quality.

SECTION VI

MATERIALS WITH IMPROVED STORAGE CAPACITY

A. INTRODUCTION

Although $LiNbO_3$:Fe has excellent storage capacity, it is clear that additional sensitivity would further enhance its usefulness. Our model for the electronic basis of hologram storage suggests two broad approaches by which increased sensitivity might be achieved in this material.

One approach is the elimination of shallow traps in $LiNbO_3$:Fe to improve the recording sensitivity. This could be accomplished as follows. The mobility of excited electrons during the write process, and hence the quantum efficiency for the writing process, appears to be limited by retrapping of the electrons in shallow traps. The traps may arise from any of the defects that are characteristic of insulating solids and are known to be particularly numerous in $LiNbO_3$. Without knowing the precise nature of the traps, it may be possible to alter their concentration sufficiently to increase the mobility of the electrons. This could be accomplished through charge compensation. Assuming that the traps are charged defects, deliberate doping of the crystal to introduce a defect with the same sign will decrease the concentration of the trap. For example, doping a $LiNbO_3$ crystal with Mo or W, which substitute for some of the Nb to form a positive charge defect, will tend to decrease the population of other positive defects (such as oxygen vacancies).

Another approach would be to provide a new set of levels, in addition to the Fe, whose purpose would be as follows. If these levels are reasonably close to the conduction band, they may impede the transport of electrons during readout, thereby rendering the crystal resistant to optical damage at room temperature. Of course, the crystal would also be less sensitive to writing at room temperature. If the traps are, however, sufficiently close to the conduction band that heating the crystal to the 100° to 200°C range will thermally ionize them in a reasonably short time, the crystal may be sensitive while hot. Some evidence for this kind of behavior exists, as is discussed later in this section.

There is, in addition, an alternative approach which is to search for dopants other than Fe to be used either singly or in combination to provide a

more sensitive system than Fe-doped $LiNbO_3$ by virtue of a higher quantum efficiency for excitation of conduction electrons.

In this section we report the results of measurements on a number of Fe co-doped $LiNbO_3$ crystals. As a result of our work on the Fe-Mn system, we were led to investigate the behavior of $LiNbO_3$ singly doped with Mn, and these results are also included in this section. Finally, because of a report on high recording sensitivity in Rh-doped $LiNbO_3$, we investigated crystals of that material and these results are also included here.

B. DOUBLE-DOPED CRYSTALS

A number of $LiNbO_3$ crystals containing Fe and another dopant were grown and evaluated. The second dopant was chosen from elements that were known or thought to participate in charge transfer processes in other oxide crystals, since these could serve either as charge compensators or a source of additional energy levels. The hologram writing sensitivity of these crystals was measured at room temperature and at 160°C. The results are shown in Fig. 15. The results for Fe-Rh, Fe-W, Fe-Mo and Fe-V are all similar to each other. They do not differ measurably from the behavior of singly doped $LiNbO_3$:Fe. The Fe-Mo sample was annealed in argon to further reduce the Fe and then re-measured. An increase in sensitivity was observed as shown in Fig. 16, but this is accounted for entirely by the increased Fe absorption. The slight temperature dependence of the sensitivity of these crystals and of singly doped $LiNbO_3$:Fe may be an indication of thermal excitation of some of the shallow trap concentration. The presence of such shallow traps is discussed in subsection D below. However, the temperature dependence of excitation from those traps would be too great (x 100 from room temperature to 160°C) to account for the slight temperature dependence seen here (10% → 50% increase) in all samples but the Mn.

A more likely explanation has simply to do with the increase in the diffusion length L with temperature as discussed in subsection F below.

The only significantly different results obtained are those for Fe-Mn. These are noteworthy for two reasons. The overall depression of the sensitivity is due to the highly oxidized state of the crystal (low Fe^{2+} concentration). However, the temperature enhancement of the sensitivity is considerably larger

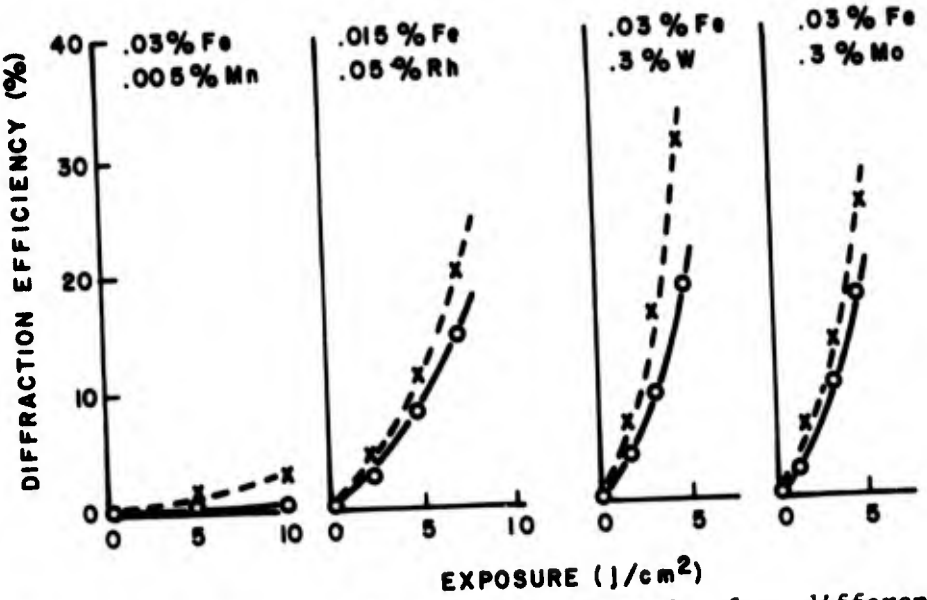

Figure 15. Recording sensitivity curves for four different double-doped $LiNbO_3$ crystals at room temperature and 160°C.

$LiNbO_3$:Fe, Mo
(PARTIALLY REDUCED)

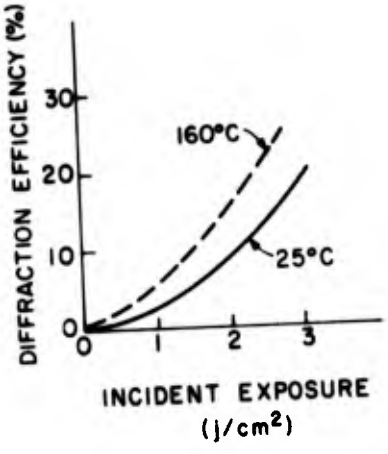

Figure 16. Recording sensitivity of Fe-Mo and Fe-V doped $LiNbO_3$ at room temperature and 160°C.

than the other materials. This type of anomalously high temperature dependence of sensitivity is also observed in crystals singly-doped with Mn and will be discussed later in this section.

C. Rh-DOPED $LiNbO_3$

Our early evaluation of hologram storage in Rh-doped $LiNbO_3$ [11] followed a description of storage in it by another group [15]. At that time we determined that the minute amount of storage we observed in our crystal could be explained easily by residual Fe. Although we suspected that the results of the other group arose from a large degree of Fe-contamination of their crystals, we could not be sure that their crystals did not differ from ours in some more fundamental way.

In light of our recent understanding of the temperature dependence of hologram storage in Fe- and Mn-doped $LiNbO_3$, we decided to reevaluate a Rh-doped crystal at different temperatures to search for evidence of a deep trap which might be empty in our samples and filled in those of the other group. The presence of such a trap would provide an excellent way to reduce the sensitivity of crystals after holograms had been written in them.

A 0.5-cm-thick crystal containing 0.05% Rh was evaluated at successively increasing temperatures from 22° to 125°C. The 22°C saturated diffraction efficiency was about 4%, and it increased very little between room temperature and 125°C. This result reinforces our original conclusion that Rh-doping induces no hologram storage properties of its own, at any temperature.

D. OPTICAL PROPERTIES OF SHALLOW TRAPS

To gain further information about shallow traps in $LiNbO_3$:Fe, the optical behavior of singly-doped crystals was investigated at low temperatures. The crystals were mounted in a Hoffman dewar equipped with a small electric heater wound around the cold finger. A plug was used to keep the liquid-nitrogen out of the bottom chamber of the dewar. The dewar was placed in a Cary spectrophotometer to obtain absorption curves of the crystals. Cooled crystals were irradiated with 3600 to 4000 Å ultraviolet light from a mercury lamp and suitable filters or with red light from the same lamp and a different set of filters. We found that whereas lightly reduced crystals showed very little change in absorption in response to these irradiations, there was a significant change in the absorption of heavily reduced crystals; this change is illustrated in Figs. 17 and 18. Ultraviolet irradiation causes a lowering of the Fe^{2+} spectrum and the appearance of a totally new absorption spectrum. The new absorption

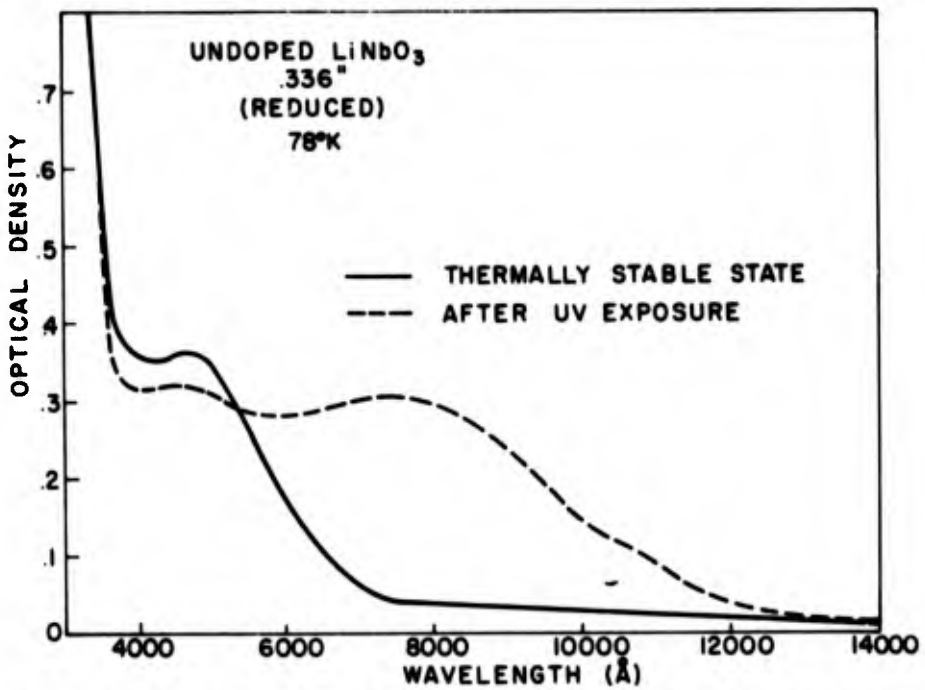

Figure 17. Optical absorption vs wavelength for reduced Fe-doped $LiNbO_3$ showing the effect of ultraviolet exposure at 78 K.

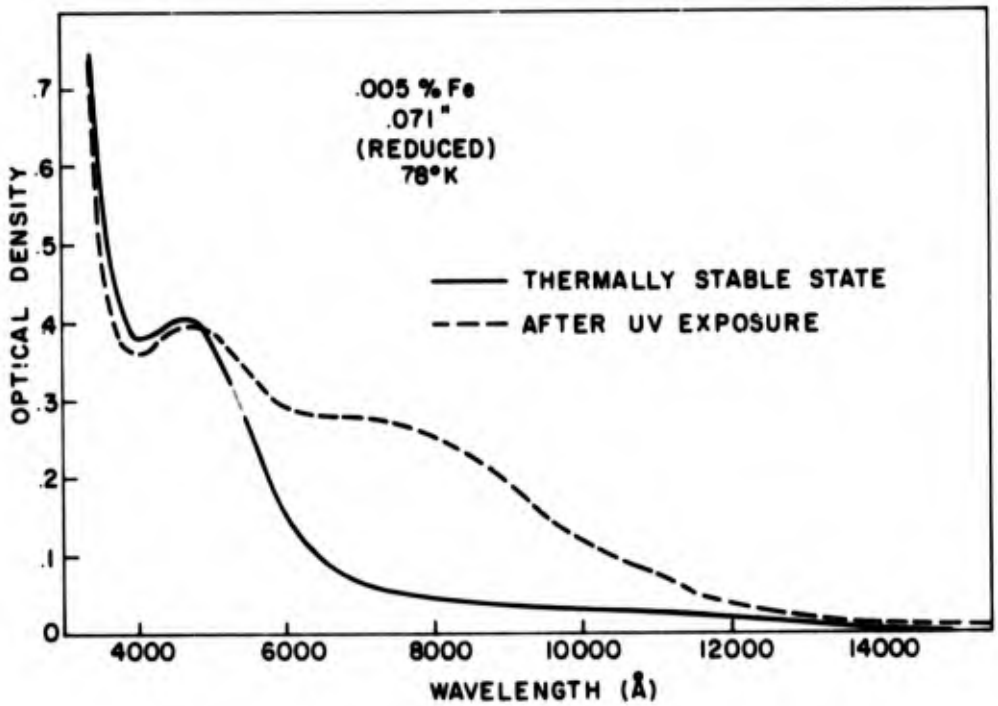

Figure 18. Optical absorption vs wavelength for nonintentionally doped $LiNbO_3$ showing effects of ultraviolet exposure at 78 K.

spectrum is relatively stable at the low temperature but decays rapidly as the crystal is heated. Direct decay time measurements were difficult to make with this setup because the dewar had to be moved to the spectrophotometer after each irradiation. Nevertheless, an approximate curve of decay constant vs temperature was observed and is shown in Fig. 19. The slope of the decay time vs 1/T curve corresponds to an activation energy $E_a \cong 0.28$ eV.

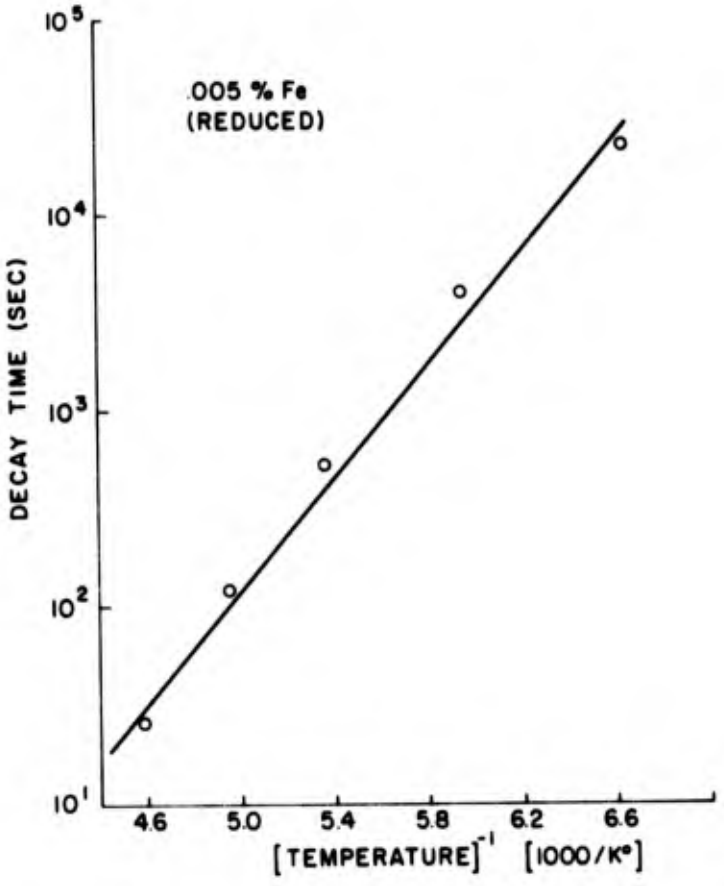

Figure 19. Decay of trap absorption vs 1000/T for ultraviolet exposed $LiNbO_3$.

When ultraviolet-irradiated crystals are irradiated with red light at 80 K, the new absorption is bleached and the Fe^{2+} spectrum reappears. However, the latter does not reach its original intensity unless the crystal is heated to room temperature.

These results can be explained if it is assumed that, at low temperature, electrons excited by ultraviolet or blue light from the Fe^{2+} ions are trapped

in the shallow traps, giving rise to the new absorption spectrum. This does not occur at room temperature because the shallow traps empty too fast. (The room temperature decay time can be estimated from Fig. 4 to be ∿300 ms.) It does not occur in heavily doped, lightly reduced crystals because there are too many Fe ions present and these compete with the shallow traps for the free electrons. From a comparison of activation energies, this trap can be identified as a Mn ion. This will be discussed more fully below.

E. Mn DOPING: RECORDING TEMPERATURE DEPENDENCE

As described earlier in this section, the recording sensitivity of crystals of $LiNbO_3$ co-doped with Rh, W, V, Mo, and Mn was measured at room temperature and at 160°C. The sensitivity for all but the Fe-Mn sample was found to increase by about a factor of 2 at 160°C as compared with room temperature. The highly oxidized Fe-Mn sample showed a much larger increase, roughly a factor of 10. When this sample was reduced to increase the Fe^{2+} concentration, the sensitivity increased and the temperature dependence became comparable to the other double-doped samples. This indicates that the temperature dependence is a property of the Mn dopant alone and not a cooperative effect between Mn and Fe. In the reduced sample, optical excitation of the Fe dominates, and the effect of the Mn is no longer seen.

Here we examine the variation in sensitivity, relaxation, and fixing as a function of the temperature in Mn-doped $LiNbO_3$ in order to try to understand what is happening in this material and the relationship of this behavior to the case of Fe-doped $LiNbO_3$.

To measure the variation in recording sensitivity with temperature, holograms were recorded at a number of different temperatures for different exposure levels. The results for 0.01 mole % and 0.1 mole % Mn are shown in Figs. 20 and 21. The difference in the obtainable diffraction efficiency between the two figures scales roughly with the optical density of the two samples. At low exposure the diffraction efficiency increases by a factor of 50 to 100 for each sample. At higher temperatures the maximum observable diffraction efficiency saturates at successively lower values due to ionic compensation or thermal erasure of the recorded grating. Figures 22 and 23 show the diffraction efficiency plotted versus $10^3/T$ (K^{-1}) for a number of different exposures.

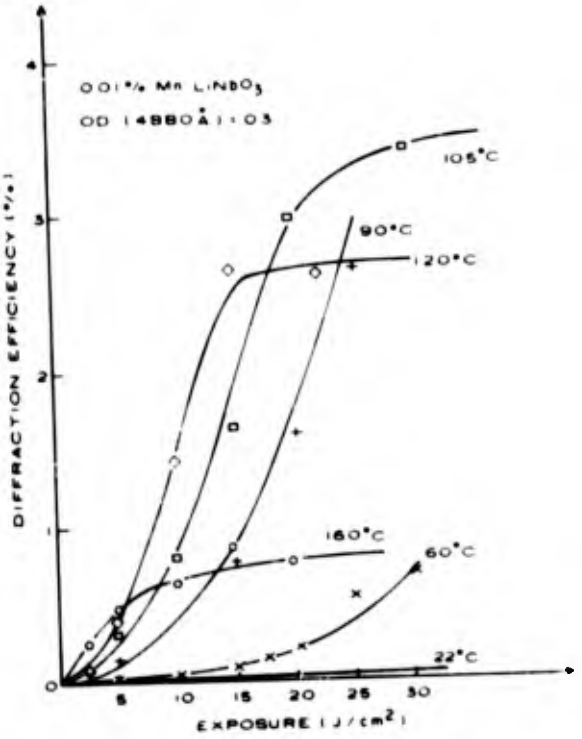

Figure 20. Diffraction efficiency vs exposure for 0.01 mole % Mn-doped $LiNbO_3$ at a number of different temperatures.

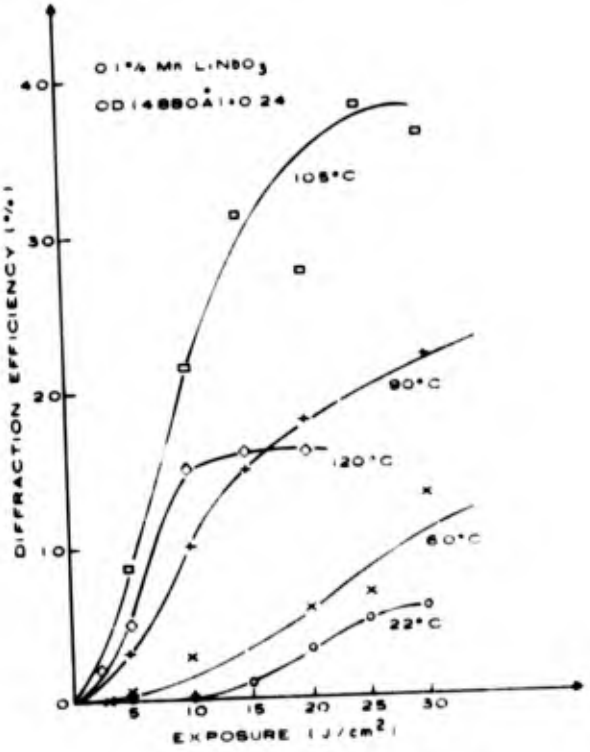

Figure 21. Diffraction efficiency vs exposure for 0.1 mole % Mn-doped $LiNbO_3$ at a number of different temperatures.

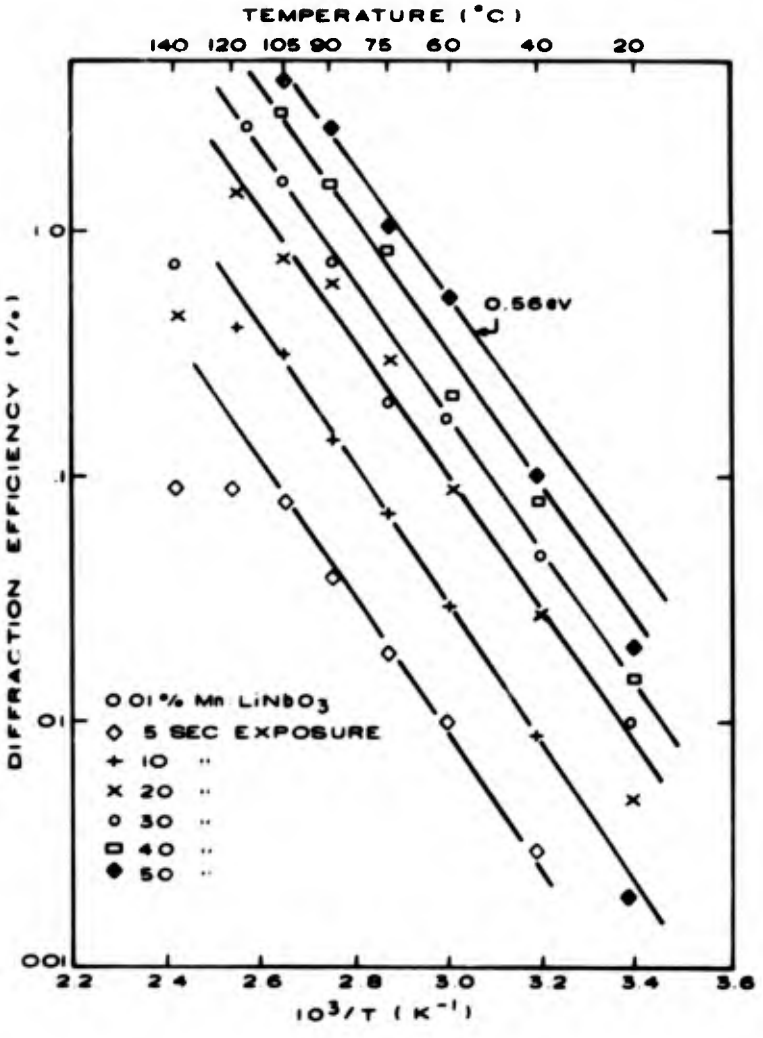

Figure 22. Diffraction efficiency vs $10^3/T$ for 0.01 mole % Mn-doped $LiNbO_3$ at a number of different temperatures.

From these curves a characteristic energy for the increase in recording sensitivity with temperature can be determined. For 0.01 mole % Mn doping, the characteristic energy is 0.56 eV; for the 0.1 mole % Mn doping, this energy is 0.48 eV.

The increase in diffraction efficiency with increasing quantum efficiency per absorbed photon Q is given by

$$\eta = \sin^2 \frac{\pi d \Delta n}{\lambda \cos\theta_B} = \sin^2 [\alpha Q] \qquad (37)$$

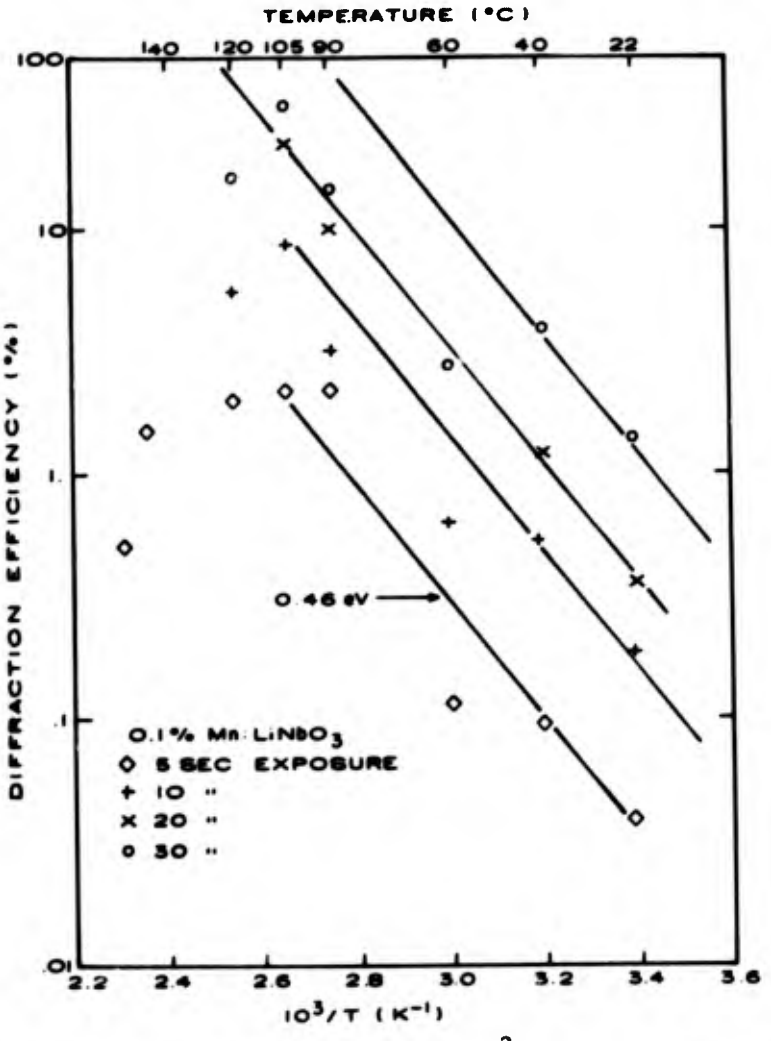

Figure 23. Diffraction efficiency vs $10^3/T$ for 0.1 mole % Mn-doped $LiNbO_3$ at a number of different exposures.

where α is a constant into which are lumped all other parameters and the index change is proportional to the exposure. From Figs. 22 and 23, we define $Q = Q_o e^{-E_a/kT}$. For small values of αQ, Eq. (37) becomes

$$\eta \sim \alpha^2 Q^2 = \alpha^2 Q_o^2 e^{-2E_a/kT} \tag{38}$$

For the two doping levels studied here, the E_a for the increase in sensitivity with temperature is 0.28 eV for the 0.01% Mn-doped sample and 0.24 eV for the activation energy of a trap associated with the Mn doping.

Optical bleaching experiments at low temperatures in 0.005 mole % Fe-doped $LiNbO_3$ which were discussed above showed the existence of a shallow trap with an activation energy of 0.28 eV. Thus, the 0.28-eV level present in

the Mn-doped sample and the heavily reduced lightly-Fe-doped material have the same thermal activation energy. These findings are either a remarkable coincidence, or we are observing the same trap in both cases.

F. Mn DOPING MODEL

If we assume that in all cases, Fe-doped, (Mn,Fe)-doped, and Mn-doped $LiNbO_3$, the trap is the same and due to a Mn level lying ~0.28 eV below the conduction band minimum, it is possible to explain the experimental results.

(1) *Observance of shallow traps at low temperature in heavily reduced Fe-doped $LiNbO_3$ (containing 10-ppm Mn as a trace contaminant).* -- Electrons excited by UV light in the reduced material are trapped at low temperature in these traps. The oxidized material does not exhibit this effect because there are too many competing Fe^{3+} sites.

(2) *Small increase in writing sensitivity with increasing temperature in Fe-doped $LiNbO_3$ used for multiple storage (heavily doped, lightly reduced).* -- Optical excitation from the Fe^{2+} sites puts electrons in the conduction band directly where transport is determined by numerous scattering mechanisms, one of which is getting caught in the Mn trap. As in (1), electrons recombine in Fe^{3+} sites before getting caught in an Mn trap. Because the diffusion length is temperature dependent, $L = \left(\frac{\mu kT}{e}\right)\tau^{1/2}$, an increase in the writing sensitivity of a factor of 1.5 should be realized at 160°C since $\eta \propto L^2$ [1]. The actual sensitivity increase observed is an almost consistent factor of 2 to 3. This suggests that in this lightly reduced material some of the Mn traps can act as recombination centers so that electrons caught in them can be lost. Increasing the temperature empties these traps before recombination takes place. This effect is small.

(3) *Large increase in recording sensitivity with temperature in (Mn, Fe)-doped, oxidized $LiNbO_3$.* -- Because the sample is not reduced, the Mn centers absorb the light. The excited electrons are trapped immediately in the Mn level at 0.28 eV, and heat (or IR radiation) is required to get reasonable sensitivity.

(4) *Small increase in sensitivity with temperature of (Mn-Fe)-doped reduced $LiNbO_3$.* -- Fe is the absorbing center, and there is a large fraction of Fe^{2+}. The Mn absorbing center lies below the Fe, and because the Fe sites are full (large fraction of Fe^{2+}), these Mn sites are full. Hence, even if the electrons excited from the Fe by light are caught in the Mn trap, there is no place to go except back into the conduction band. The transport is slowed down, but the sensitivity is not reduced.

(5) *Large temperature dependence of sensitivity in Mn-doped $LiNbO_3$.* -- Electrons excited from the Mn center need heat to escape into the conduction band as in (3).

It is possible to interpret all of these features without incorporating a trap on the Mn. However, for the experiments described, the trap has the features identical to those expected for a trap on the Mn site. We have, therefore, tentatively identified the traps which are controlling the temperature dependence of the sensitivity as Mn traps 0.28 below the conduction band edge. We have shown that the enormous temperature dependence results when Mn is used as the absorbing center. The implication of these results for the Mn ion is that the holographic storage medium can be prepared with a variable sensitivity. A low sensitivity for room temperature readout and a high sensitivity at the recording temperature would be extremely valuable in that it would significantly reduce the buildup of optical damage. The investigation of hologram storage and decay in Mn-doped crystals at elevated temperatures is described below.

G. Mn DOPING: HOLOGRAM DECAY AT ELEVATED TEMPERATURES

Holograms were recorded at a variety of different temperatures in Mn-doped samples, as shown in Figs. 20 and 21. At any temperature the hologram will "decay" by ionic compensation (fixing) or by actual thermal erasure. At room temperature the time constant of both these effects is very long. In Fig. 24 the time dependence for the recording and decay of a hologram at 120°C is shown. In Fig. 25 the time constant for the decay of holograms in the dark is shown for a variety of different temperatures and two levels of Mn doping. The activation energy is measured to be 1.22 eV for the 0.1% doping level and 1.23

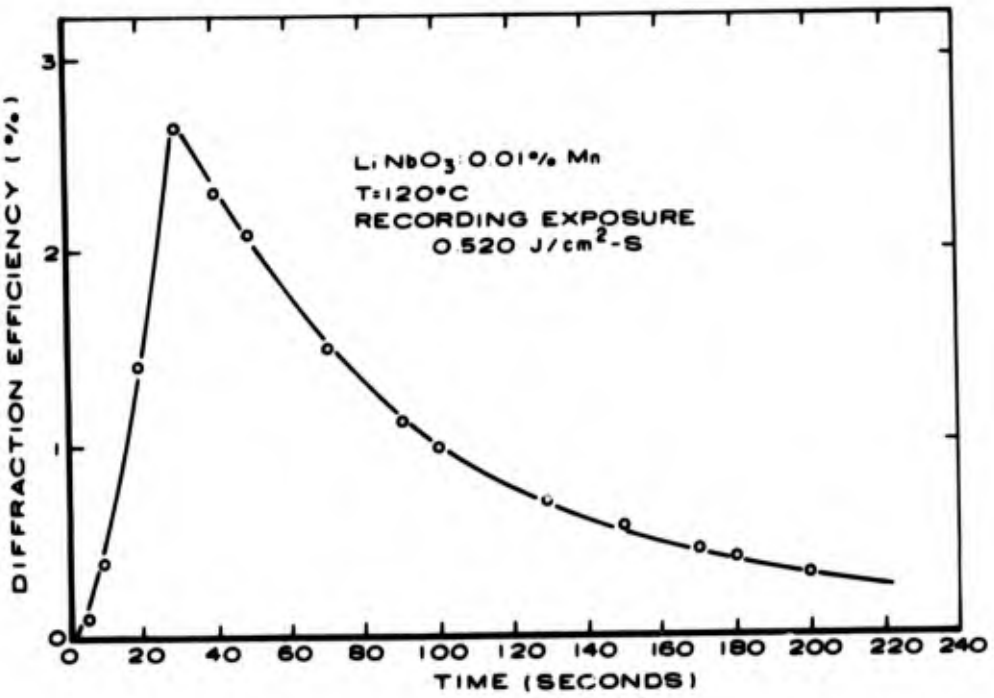

Figure 24. Recording sensitivity and ionic relaxation after storage ends for 0.01 mole % Mn-doped $LiNbO_3$.

eV for the 0.001% doping level. There is no significant difference between these results. The 1.18-eV activation energy for ionic relaxation and the 1.48-eV activation energy for thermal erasure in Fe-doped samples are also shown on Fig. 25. The experiments reported here cannot distinguish between fixing and thermal erasure, but the close similarity of the observed activation energies in the Fe-doped and Mn-doped samples indicate that we are observing the ionic relaxation process.

Thermal erasure should have an excitation energy characteristic of the Mn centers, which are deeper than the Fe sites. Therefore, the activation energy should be even higher than 1.48 eV and the thermal erase line even steeper.

The results presented above would indicate that we should be able to fix holograms in Mn-doped samples with the same efficiency as is the case with the Fe-doped samples. We have recorded high-efficiency holograms at temperatures of 150°C and 160°C but have only been able to fix ∿1% efficient holograms. We have also recorded holograms at 100°C, then heated the sample to 160°C for a

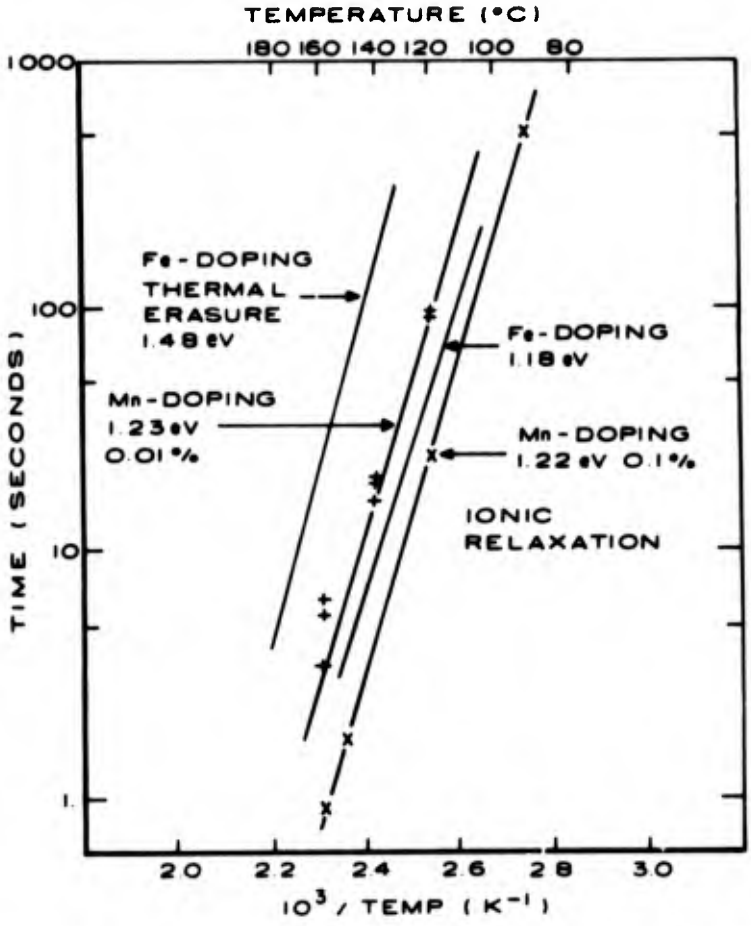

Figure 25. Time constant for ionic relaxation vs $10^3/T$ at two different Mn doping levels. Also shown for comparison are previously measured curves for ionic relaxation and thermal erasure in Fe-doped $LiNbO_3$.

few minutes, and then cooled the sample to room temperature. Again, we have only been able to fix ∿1% efficient holograms.

H. Mn DOPING: OPTICAL BEHAVIOR

It was known from earlier work [1] that oxidation could increase the intensity of the 5770 Å absorption peak of Mn-doped $LiNbO_3$ (see Fig. 26) rather than decrease it as would be the case for Fe-doped $LiNbO_3$. However, strong oxidation is found to nearly eliminate the visible absorption of a crystal doped with 0.01% Mn, as is shown in the lower curve of Fig. 27. One explanation for this behavior is that there may be three valence states in which Mn

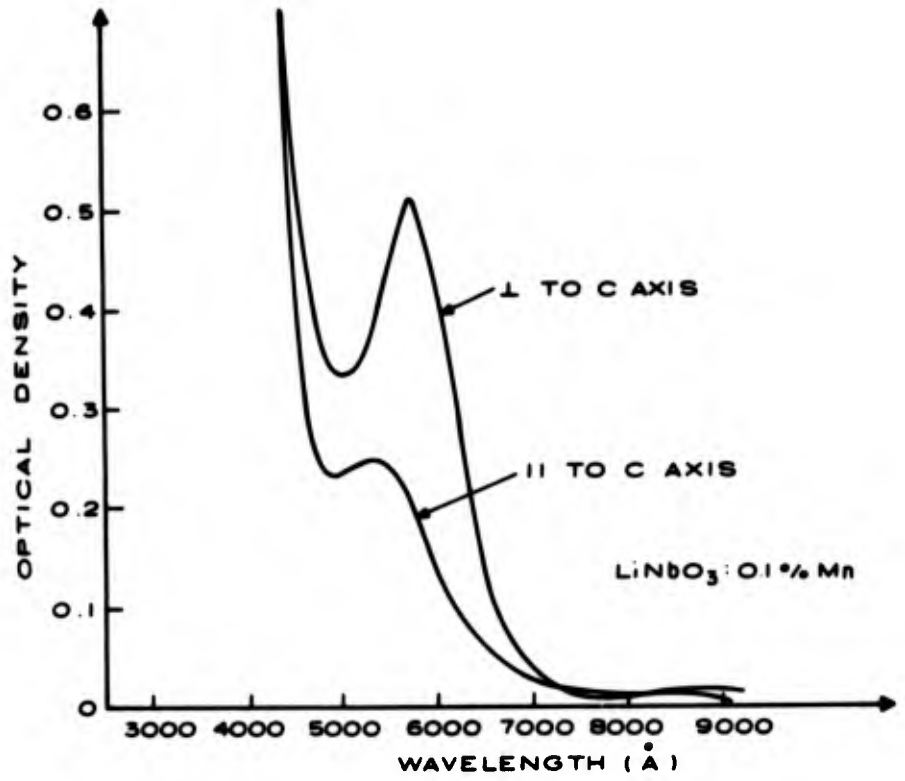

Figure 26. Typical Mn spectra in $LiNbO_3$.

can be stabilized and that the "middle" state produces the peak at 5750 Å. An additional state of the crystal was produced by argon annealing the 0.01% Mn-doped crystal at 1140°C and then quenching it rapidly to room temperature. The result of this procedure is shown in the upper curves of Fig. 27. The spectra produced seem to bear no resemblance to Fig. 26 and probably represent Mn in its lowest valence state.

These optical spectra most likely arise from several different valence states of the Mn ion. The contributions of these different valence states cannot be sorted out at this time since we know neither the valence states involved nor the optical spectra of particular valence states.

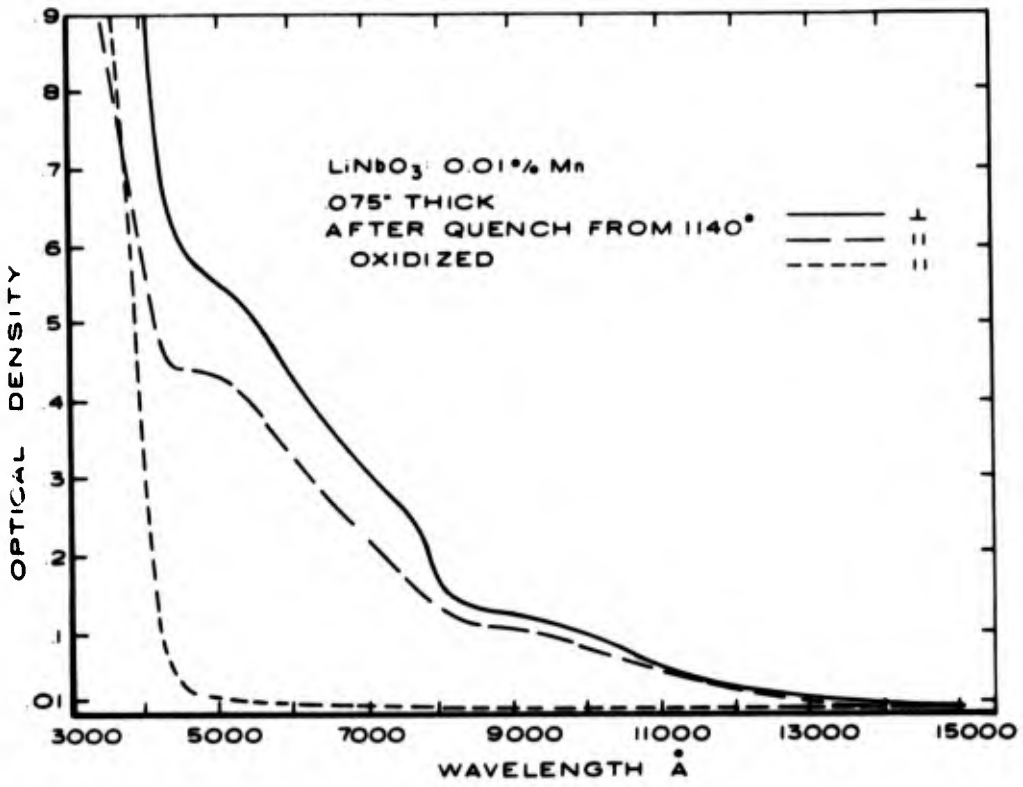

Figure 27. Optical absorption spectra of Mn-doped $LiNbO_3$ after heavy oxidation and after heavy reduction.

SECTION VII

SUMMARY AND CONCLUSIONS

We have found Fe-doped $LiNbO_3$ to be the best candidate for a volume holographic storage medium [1,2,3]. During 1974 our effort was concentrated on the development of a better understanding of the recording, erasure, and fixing behavior of Fe-doped $LiNbO_3$ at elevated temperatures and development of methods to improve the material performance. We have permanently recorded 500 holograms with diffraction efficiencies greater than 5% in Fe-doped $LiNbO_3$.

The drift-like nature of the recording process at elevated temperatures was confirmed. Experimental studies of the bulk photovoltaic effect in Fe-doped $LiNbO_3$ led to the development of a model to explain the origin of the apparent internal electric field. A model for the hologram erasure process at high temperatures was also developed and tested. The coupling of these results led to the prediction that the erase/record asymmetry increases linearly with the empty trap (Fe^{3+}) concentration. This prediction is in agreement with our earlier observation of unexpectedly large asymmetry in 0.02% Fe-doped $LiNbO_3$ crystals.

The bulk photovoltaic effect is due to the unidirectional transport of charge. At elevated temperatures the mobile ionic species which enables us to fix holograms in Fe-doped $LiNbO_3$ will follow this electronic transport. Using these facts we identified Si as a mobile ion in $LiNbO_3$. An increase in the Si ion concentration, if Si is the dominant mobile ion, should permit a reduction in the recording temperature thus reducing the thermal erasure. This same approach may also be useful in other applications of $LiNbO_3$ where optical damage occurs. In such cases, an ionic species which is mobile at the operating temperature would compensate the buildup of electronic space-charge field in the material.

The investigation of other dopants to improve the material performance led to the discovery of Mn-doped $LiNbO_3$. In this material the recording sensitivity increases by a factor of fifty at 120°C compared with that at room temperature. The significance of this result is that the recording medium could be prepared with a optical sensitivity which can be varied between recording and readout. This could lead to a significant reduction in the buildup of spurious optical damage on readout.

This work has led to an understanding in detail of the mechanisms of hologram storage in $LiNbO_3$. This understanding has led to the development of techniques for the permanent storage of 500 holograms with ~5% efficiency in Fe-doped $LiNbO_3$. The recent discoveries point the way to increases in capacity which make the Fe-$LiNbO_3$ recording system limited only by fundamental optical principles, not material parameters.

REFERENCES

1. D. L. Staebler, W. Phillips, and B. W. Faughnan, *Materials for Phase Holographic Storage (U)*, Final Report, Contract N00019-72-C-0147, prepared for Naval Air Systems Command, March 1973.
2. D. L. Staebler, W. Phillips, W. Burke, and B. W. Faughnan, *Materials for Phase Holographic Storage (U)*, Final Report, Contract N00019-73-C-0273, prepared for Naval Air Systems Command, February 1974.
3. W. Burke and D. L. Staebler, *Volume Holographic Material Device Feasibility for Map Display Applications*, Final Report, Contract N62269-72-C-0793, prepared for Naval Air Development Center, June 1973.
4. D. L. Staebler and J. J. Amodei, Ferroelectrics 3, 107 (1972).
5. For example, Shyh Wang, *Solid State Electronics* (McGraw-Hill, New York, 1966), p. 274.
6. W. Phillips and D. L. Staebler, J. Elect, Materials 3, 601 (1974).
7. W. Phillips, J. J. Amodei, and D. L. Staebler, RCA Review 33, 94 (1972).
8. D. L. Staebler and W. Phillips, Appl. Opt. 13, 788 (1974).
9. F. S. Chen, J. Appl. Phys. 40, 3389 (1969).
10. D. L. Staebler and J. J. Amodei, J. Appl. Phys. 43, 1042 (1972).
11. J. J. Amodei and D. L. Staebler, RCA Review 33, 71 (1972).
12. M. G. Clark, F. J. DiSalvo, A. M. Glass, and G. E. Peterson, J. Chem. Phys. 59, 6209 (1973).
13. N. F. Mott and R. W. Gurney, "Electronic Process In Ionic Crystals," (Oxford University Press, London, 1951), p. 26.
14. J. J. Amodei, RCA Review 32, 185 (1971).
15. A. Ishida, O. Mikami, S. Miyazawa, and M. Sumi, Appl. Phys. Lett. 21, 192 (1972).

APPENDIX A

TIME CONSTANT FOR ERASURE

In this appendix we derive the solution to the problem of thermal erasure considering only diffusion.

The holographic pattern is due to the difference between the electronic and ionic charge patterns. Exposure to uniform light after fixing with ions allows some redistribution of the electrons. The space-charge field of the ions does not allow a complete redistribution, however. At high temperature, the electrons redistribute, the ionic pattern follows the moving electrons, and the pattern disappears. Therefore, for calculating the erasure we consider only the redistribution of the electronic charge.

The number of trapped electrons (ρ), different from the equilibrium (no pattern) value, at $t = 0$ is

$$\rho(x_1) = \rho_o \sin Kx \tag{A-1}$$

where $K = \frac{2\pi}{\ell}$ and ℓ is the grating spacing.

The number of electrons in the conduction band $n(x,t)$ has the following time dependence:

$$\frac{\partial n(x,t)}{\partial t} = g\rho\ (x,t) - \frac{n(x,t)}{\tau} + D\,\frac{\partial^2 n(x,t)}{\partial x^2} \tag{A-2}$$

where g is the generation rate per filled trap, τ is the lifetime of the excited electrons, and D is the diffusion constant.

The time rate of change of the filled trap density is

$$\frac{\partial \rho(x,t)}{\partial t} = -\,g\rho(x,t) + \frac{n}{\tau} \tag{A-3}$$

There is no diffusion among the traps.

We assume

$$n = A(t) \sin Kx \tag{A-4}$$

$$\rho = B(t) \sin Kx \tag{A-5}$$

Then using Eqs. (A-2) and (A-3)

$$A' = gB - \frac{A}{\tau} - DK^2 A \tag{A-6}$$

and

$$B' = -gB + \frac{A}{\tau} \tag{A-7}$$

where A and B are functions of t. We suppose A and B are of the form

$$A = A_o e^{-\alpha t}, \tag{A-8}$$

$$B = B_o e^{-\alpha t} \tag{A-9}$$

Then

$$\left(-\alpha + \frac{1}{\tau} + DK^2\right) A - gB = 0 \tag{A-10}$$

$$-\frac{1}{\tau} A + (-\alpha + g) B = 0 \tag{A-11}$$

For this system of coupled equations to have a solution, the determinant of the coefficients must be zero or

$$\alpha = \frac{1}{2}\left(g + \frac{1}{\tau} + DK^2\right) \pm \frac{1}{2}\sqrt{\left(g + \frac{1}{2} + DK^2\right)^2 - 4\, DK^2 g} \tag{A-12}$$

Using the binomial series expansion for the square root

$$\alpha \cong \frac{1}{2}\left(g + \frac{1}{\tau} + DK^2\right) \pm \frac{1}{2}\left(g + \frac{1}{\tau} + DK^2\right)\left(1 - \frac{2\, DK^2 g}{\left(g + \frac{1}{\tau} + DK^2\right)^2}\right) \tag{A-13}$$

$$\alpha_+ = g + \frac{1}{\tau} + DK^2 - \frac{DK^2 g}{g + \frac{1}{\tau} + DK^2} \tag{A-14}$$

$$\alpha_- = \frac{DK^2 g\tau}{1 + g\tau + DK^2\tau} \tag{A-15}$$

For

$$g \lesssim 1\ s^{-1} \qquad \text{(See appendix B)}$$

$$\tau = 10^{-11}\ s$$

$$D = 0.02\ cm^2/s$$

$$K = 6 \times 10^4/cm$$

We have

$$\alpha_+ \cong g + \frac{1}{\tau} + DK^2 = 10^{11}/s \tag{A-16}$$

$$\alpha_- = DK^2 g\tau = 7 \times 10^{-4}/s \tag{A-17}$$

Therefore

$$n(x,t) = \left(A_o^+ e^{-\left(g + \frac{1}{\tau} + DK^2\right)t} + A_o^- e^{-\left(DK^2 g\tau\right)t} \right) \sin Kx \tag{A-18}$$

$$\rho(x,t) = \left(B_o^+ e^{-\left(g + \frac{1}{\tau} + DK^2\right)t} + B_o^- e^{-\left(DK^2 g\tau\right)t} \right) \sin Kx \tag{A-19}$$

Substituting into Eq. (A-7)

$$A_o^- = +B_o^- \left(g - DK^2 g\tau\right)\tau \tag{A-20}$$

and

$$A_o^+ = -B_o^+ \left(\frac{1}{\tau} + DK^2\right)\tau \tag{A-21}$$

The initial conditions at t = 0,

$$n = 0 \tag{A-22}$$

$$\rho = \rho_o \sin Kx \tag{A-23}$$

Imply

$$A_o^+ = -A_o^- \tag{A-24}$$

$$B_o^+ + B_o^- = \rho_o \tag{A-25}$$

Therefore from Eqs. (A-20), (A-22), (A-24), and (A-25)

$$B_o^+ = \frac{\rho_o}{1 + \dfrac{1 + DK^2\tau}{g\tau(1 - DK^2\tau)}} \tag{A-26}$$

$$B_o^- = \frac{\rho_o}{1 + \dfrac{g\tau(1 - DK^2\tau)}{1 + DK^2\tau}} \tag{A-27}$$

$$A_o^+ = \frac{-\rho_o}{\dfrac{1}{1 + DK^2\tau} + \dfrac{1}{g\tau(1 - DK^2\tau)}} \tag{A-28}$$

$$A_o^- = - A_o^+ \tag{A-29}$$

Since $DK^2\tau \sim 10^{-3}$ and $g\tau \sim 10^{-11}$

$$B_o^+ \approx \rho_o g\tau \tag{A-30}$$

$$B_o^- \approx \rho_o \tag{A-31}$$

$$A_o^+ \approx -\rho_o g\tau \tag{A-32}$$

$$A_o^- \approx \rho_o g\tau \tag{A-33}$$

The complete solution for the time dependence of the trapped charge is then

$$\rho(x,t) = \left[\rho_o g\tau\, e^{-\left(g + \frac{1}{\tau} + DK^2\right)t} + \rho_o\, e^{-\left(DK^2 g\tau\right)t}\right] \sin Kx \tag{A-34}$$

The first term decays in less than 10^{-11} s and is the transient resulting from the initial condition n = 0 at t = 0. The second term provides the time constant for the slow decay of the pattern

$$\tau = \frac{1}{DK^2 g\tau} \tag{A-35}$$

APPENDIX B

THERMAL AND OPTICAL GENERATION RATES

here we estimate the magnitude of the generation rate of free electrons g per trap for electrons trapped on an Fe^{3+} ion in $LiNbO_3$.

For optical excitation

$$g_o = \frac{I_o \sigma}{\hbar\omega} \tag{B-1}$$

where I_o is the incident light intensity/cm^2, σ is the light absorption cross section for the electron, and $\hbar\omega$ is the photon energy. In a 1-cm-thick crystal we control the Fe^{2+} concentration so that an absorption coefficient α of 0.7 cm^{-1} is achieved, giving 50% absorption. Since $\alpha = \sigma N$ where N is the number of trapped electrons, $N \approx 10^{17}/cm^3$, then the absorption cross section $\sigma \approx 7 \times 10^{-18}$ cm^2. For $I_o = 0.1$ W/cm^2 and $\hbar\omega = 4 \times 10^{-19}$ joules/photon for 5000 Å light:

$$g_o \approx 2\ s^{-1} \tag{B-2}$$

For thermal erasure the generation rate g_t per trap is

$$g_t \approx \nu e^{-E_a/kT} \tag{B-3}$$

where $E_a \approx 1.48$ eV is the thermal activation energy and ν is the vibrational frequency of an electron in its potential well. For $\nu \approx 10^{15}$ s^{-1}

$$g_t \approx 2 \times 10^{-3}\ s^{-1} \tag{B-4}$$

Another estimate of the thermal erasure rate can be obtained from the data presented in Fig. 3 in the main body of this report. For typical operating conditions of $\ell = 0.94$ μ, a concentration of 0.015% and a temperature of 160°C, the time constant for thermal erasure is: 5×10^3 s. From Eq. (3) in the report the time constant is

$$T = \left\{ DK^2\, g_t \tau \right\}^{-1}$$

or the generation rate is

$$g_t = \left\{ DK^2 T \tau \right\}^{-1}$$

For $D = 0.02\ cm^2/s$, $K = 6.7 \times 10^4$ and $\tau = 10^{-11}\ s$.

$$g_t \gtrsim 0.2\ s^{-1} \tag{B-5}$$

The values of the generation rate per trap are, therefore, $\lesssim 1$ for both optical or thermal processes.